Université Libre de Bruxelles

Faculté des Sciences Appliquées

Updating Acoustic Models : a Constitutive Relation Error Approach

Vincent Decouvreur

Dissertation originale présentée en vue de l'obtention du grade de Docteur en Sciences Appliquées

Année académique 2007-2008

Updating Acoustic Models : a Constitutive Relation Error Approach

Vincent Decouvreur

Directeurs de thèse :

Pr. Philippe Bouillard

Building, Architecture
and Town planning Dept.
Université Libre de Bruxelles
Belgium

Pr. Pierre Ladevèze

Laboratoire de Mécanique
et Technologie
ENS-Cachan Paris VI/CNRS
France

Thèse de doctorat financée par le FRIA, Fonds pour
la formation à la Recherche dans l'Industrie et dans l'Agriculture

Contents

Introduction

In last decades, numerical simulation tools aiming at predicting the physics surrounding the human being were developed faster and faster. While first trials made use of computers of the size of an office and less performing than today's pocket calculators, nowadays computation centers proceed to massive parallel numerical simulations using hundreds of processors for model size of millions of degrees of freedom (see [RR00]). From that point of view, it is clear that major improvements were achieved in the computational capability domain.

In spite of it, one observes that many industry sectors are still mainly relying on experimental testing, and that computer aided predictions are often of little use in the practice, at least when both experimental and numerical testing are made available.
Actually, it looks like improvements in the computational capacity were not accompanied by a similar research interest in the physical model description area. Consequently, while extremely sophisticated machines are used to run very large numerical models, facing the numerically predicted results to experimental data remains a very challenging task.
Part of this challenge can be solved thanks to the fundamental research. Indeed, it aims at understanding the physics of those many phenomena that have still to be described by the use of either empirical laws or very simplified mathematical relations in the numerical models. Therefore, fundamental research should be promoted more than ever.

A dedicated science addresses the gap between experimental testing and numerical predictions: it is the domain of error estimation and related updating and validation techniques. Such investigation area is intrinsically of great interest since updating techniques marry experiments with numerical predictions, while today's industry behavior often tends to make them competing. This

document focuses on reconciling numerically predicted acoustic fields with corresponding experimental testing results.
The work is made harder because neither the numerical predictions nor the experimental data describe perfectly the reality, each of those models being biased by its own kinds of error (see for example [Bal97, BADM06]).
From the numerical side, the deviation with respect to reality is caused by the simplification of the geometry, (which is sometimes combined with a poor discretization of the continuous domain), the assumptions and approximations in the models describing the physics (non linearity, dissipative effects, structural joints, ...), and the identification of the coefficients describing the model (e.g. acoustic admittance model parameters).
As to the experimental part, the available information is restricted by the number of sensors and the frequency sampling that is recorded. Furthermore, experimental data are polluted by measurement noise. Despite its deviation to reality, experimental information is commonly regarded as the reference, and the updating technique is wished to be able to filter the noise and to alleviate the lack of knowledge of the discrete numerical model.

From an industrial point of view, updating techniques are used in two different contexts. The first application tends to shorten the time to market of new products during their development from virtual sketching to mass production. The updating step target is to improve the numerical model thanks to experimental testing performed on a first prototype. The updated model will provide more reliable output leading to a better next candidate, which will speed up the product development process by driving down the number of iterations of the prototyping stage. The second application is related to industry sectors where the number of prototypes to be built is kept to a few samples for either economical or technical reasons. Astronautics is a good guest for such a kind of expensive application. Additionally, many rocket properties can not be measured due to technical reasons like ambient atmosphere, including temperature/speed/stresses unpredictable combination for instance. For such cases, numerical predictions (conducted with an as reliable as possible model) are of prime importance.

Various updating techniques are developed in the literature. The way those are classified follows either the type of correction applied to the system (global or local corrections), the type of experimental information (static versus modal data, temporal versus frequency response function), or the kind of function to be minimized, which can be built on input, output, or constitutive laws.
A short literature review about existing updating techniques is presented in

section 1.2. The present work focuses on a parametric updating method based on the constitutive law error, which was extensively studied from the beginning of the eighties and successfully applied to structural dynamics ([Lad98, Der01, CLP97, Com00]). Please note that we will use indifferently the acronym CLE (Constitutive Law Error) or CRE (Constitutive Relation Error) when referring to the updating method built on the corresponding error estimator. This updating technique shows strong mechanical foundation and the analogy between acoustics and structural dynamics mathematical formulation (see section 1.1) helped believing in the potential success of applying the constitutive law error method to our favorite domain.

The objectives of the document can be summarized as follows. First, the literature on acoustic updating technique being pretty light, and the industrial interest in getting a reliable numerical tool for predicting acoustic fields increasing, addressing systematically the problem by applying a successful story from structural dynamics looks pertinent. Second, while acoustic data are potentially noisy and dispersion effect is inherent to the Helmholtz wave equation ([DBB99]), the CLE updating method will be applied to the acoustics and its robustness with respect to noise and dispersion will be evaluated. With a view to make the new technique able to improve large industrial acoustic models, effort will be spent to fasten the process, notably by reducing the problem size by projecting it into a sub-space. Finally, the CLE validation method could be used for improving the absorbing characterization of acoustic dampers. Indeed, the Kundt tube setup which is standardly used to measure acoustic properties of a sample of material located at the tube extremity is unidimensional and records the response of the sample to waves propagating perpendicularly to its surface. Using the CLE concept to update the acoustic pressure field in a fully tridimensional measurement device (instead of a wave guide) should better characterize the studied absorbing material.

The thesis manuscript is built on a skeleton made of four papers that were either published or accepted for publication in international scientific journals. After a brief introduction to the acoustics mathematical description in the frequency domain and the similitude of its formulation with structural dynamics through chapter 1, a literature review of existing updating methods is presented.
Chapter 2 describes the updating method and its application to the acoustics into details. The constitutive relation error estimator is deducted from the less reliable information of the model. So, the equations of the numerical model together with the experimental data are classified into reliable and less reliable

information. The reliable part has to be satisfied exactly, which yields to an admissible solution set. Then, the updated parameters are the ones characterizing the less reliable laws. The best admissible solution minimizes the constitutive relation error. Taking into account the experimental uncertainty contribution adds a supplementary term to the model quality estimator that becomes the modified constitutive relation error. The less reliable data are exactly verified if the estimator equals zero at the end of the updating step. The technique is applied on a 2D academic setup, and the robustness of the method with respect to measurement noise is established.
Chapter 3 examines the updating quality in presence of dispersion error that pollutes the Helmholtz equation solution when increasing the frequency ([BI99, IB95]). Note that many authors investigated the dispersion phenomenon. Some papers propose a stabilization for the finite element method ([FFML97, HH92]), while other authors focus on high order numerical approximation methods based either on the hp-formulation of the FEM ([GD96]) or on meshless techniques ([BS98, LBV03]). Today's most promising results are obtained by incorporating solution information into the numerical discrete subspace. Several formulations take advantage of this idea, like the Trefftz based approach ([CJZ91, DvHS02]), the discontinuous Galerkin FEM ([FHF01]), the variational theory of complex rays ([LARB01]), or the generalized FEM and some meshless approaches ([BM97, DBVB05]) for example.
Chapter 3 also demonstrates the updating of admittance coefficients describing the absorption in the acoustic medium through a large frequency range, whilst the dispersion error is controlled. For medium to high wave number, using a numerical approximation method exhibiting a robust frequency behavior (here the element-free Galerkin method) is shown to be more efficient than the conventional finite element method.
Chapter 4 addresses the extension of the CLE technique to 3D acoustic problems. The updating equation system to be solved being larger than the initial one, and the optimization process being iterative, solving large industrial problems requires diminishing the model size. The equation system is projected in a subspace making use of a reduced modal basis. The system is rewritten under the form of undamped forced vibration problems. The reduced basis is made of eigenmodes and series of Krylov vectors associated with the excitation of the undamped forced vibration problems. Furthermore, static responses to the forces related to the variations of the system during the updating process together with responses associated to measured degrees of freedom are additional contributions to the particular projection basis. The reduced basis is

successfully tested on an academic 3D car mesh by comparing the updated pressure fields resulting from the full and reduced numerical models.
Then, chapter 5 of the thesis presents a two-stage approach for the application of the CLE updating technique to the characterization of absorbing material properties. The updating process focuses on the wall admittance modeling for the absorbing materials which damp the sound pressure level. The idea consists in splitting the optimization run into two parts. The first part only looks for the best complex number describing each absorbing material, which is achieved for a few frequencies spread in the range of interest and independently of any admittance model. The second stage needs to select an admittance model for the frequency description of each material, and interpolates the discrete complex numbers found through stage one to get continuous material damping properties. The two-stage method is validated on a simple academic setup, and then applied to the TRICARMO concrete car cabin developed by LMS International.
The concluding chapter 6 summarizes the main findings of the thesis and proposes extending the scope of the research from cavity acoustics to open exterior domains. Concerning future developments, additional works could combine structural properties of the domain boundary with acoustic fields of the cavity, the vibro-acoustic system allowing to update either acoustic or structural dynamics properties based on coupled data. As it was already mentioned, updating in acoustics benefits from similar advances in structural dynamics, which suggests investigating new developments from recent findings in that area.
Then, the newly developed Extended Constitutive Relation Error estimator enabling to validate structural dynamics models in presence of uncertainties ([DLR04, LPDR06]) should be considered.
Recent theories propose strategies to reduce the lack of knowledge (LOK) in model validation by propagating throughout the mechanical model the bounds of uncertain LOK variables that are defined for each substructure [LPR06b, LPR06a].

Chapter 1

Acoustic updating techniques: state of the art and structural dynamics similarity

Contents

1.1 Acoustics versus structural dynamics wave equation formulation

Addressing acoustic problems takes advantage of preliminary having a look at corresponding developments in the structural dynamics area.
Indeed, based on the similarity between both mechanical domain mathematical formulations, one could use some hints from previous structural dynamics investigations. It is also the case for the constitutive law error theory that was first developed for structural applications.

To help understanding how close both investigation areas are, the temporal movement equations ([MO95]) are presented for structural dynamics (1.1) and acoustics (1.2):

$$[M_s]\{\ddot{u}\} + [B]\{\dot{u}\} + [K_s]\{u\} = \{f_s\}, \tag{1.1}$$

$$[M_f]\{\ddot{p}\} + [C]\{\dot{p}\} + [K_f]\{p\} = \{f_f\}, \tag{1.2}$$

where $[M]$ and $[K]$ are the mass and stiffness matrices of the system respectively, and subscripts $(.)_s$ and $(.)_f$ stand for structure and fluid. The damping matrix is usually named $[B]$ in structural dynamics, and $[C]$ in acoustics. The unknown vector is the displacement $\{u\}$ in structural dynamics, and the sound pressure $\{p\}$ in acoustics; the system excitation is represented by the force vector $\{f_s\}$ for the structural part and $\{f_f\}$ acts for the acoustic sources of the fluid domain (e.g. surrounding boundary vibrations, loudspeakers, ...).

In the frequency domain, equations (1.1) and (1.2) become respectively:

$$\left([K_s] + \mathrm{j}\omega[B] - \omega^2[M_s]\right)\{U\} = \{F_s\}, \tag{1.3}$$

$$\left([K_f] + \mathrm{j}\omega[C] - \omega^2[M_f]\right)\{P\} = \{F_f\}, \tag{1.4}$$

where

$$\mathrm{j} = \sqrt{-1}, \tag{1.5}$$

$$\{u\} = \{\boldsymbol{U}\} e^{\mathrm{j}(\omega t - \Phi)} = \{U\} e^{\mathrm{j}\omega t}, \tag{1.6}$$

$$\{p\} = \{\boldsymbol{P}\} e^{\mathrm{j}(\omega t - \Phi)} = \{P\} e^{\mathrm{j}\omega t}, \tag{1.7}$$

$$\{f_k\} = \{\boldsymbol{F_k}\} e^{\mathrm{j}(\omega t - \Psi)} = \{F_k\} e^{\mathrm{j}\omega t} \qquad (k = f, s). \tag{1.8}$$

In equations 1.6 to 1.8, where t is the time and ω the angular frequency while Φ and Ψ represent phase angles, it is shown that both the unknown vectors $\{U\}$

and $\{P\}$ and the excitations $\{F_s\}$ and $\{F_f\}$ contain the information about the amplitude and the phase.

Comparing equations 1.3 and 1.4 clearly identifies the similarity between both application domains. Though, some important differences are to be highlighted:

- the frequency range of interest is generally much larger in acoustics. Indeed, while the low frequency modes are of primary importance in structure computations, sounds are always filtered through the ears of the human being, which filter emphasizes non linearly frequencies belonging roughly to the 20-20000 Hz bandwidth;
- the structural dynamics damping matrix $[B]$ addresses the whole structure volume while the acoustic matrix $[C]$ applies on the surface bounding the domain. As a consequence, the updating process is sometimes split into two stages in structural dynamics, the first being dedicated to locating the most polluted regions (the ones that will be updated through the second stage) based on an error map; in acoustics, the badly defined regions are generally located around the absorbing materials.

The first interest in comparing acoustics to structural dynamics concerns the available references in the literature. Indeed, whilst there are numerous of structural dynamics works dealing with updating techniques, acoustics updating literature is pretty rare. In what follows, the updating technique review is based on those structural dynamics works, assuming that the conclusions should be applicable to the acoustics, possibly with some slight modifications. Furthermore, this work being the first one to apply the constitutive law error to the acoustics, it took advantage of the conclusions coming from the previous analyses achieved by several PhD students during their stay at the Ecole Normale Supérieure of Cachan (Paris) ([Der01, Cho97, Com00]), which boosted the developments of the technique to the cousin area of the structural dynamics.
Going one step further, one can think about updating a coupled vibro-acoustic model [MO95] that would look like system 1.9.

$$\begin{bmatrix} [K_s] + \mathrm{j}\omega\,[B] - \omega^2\,[M_s] & [K_{sf}] \\ [K_{fs}] & [K_f] + \mathrm{j}\omega\,[C] - \omega^2\,[M_f] \end{bmatrix} \begin{Bmatrix} U \\ P \end{Bmatrix} = \begin{Bmatrix} F_s \\ F_f \end{Bmatrix}, \quad (1.9)$$

where $[K_{sf}]$ and $[K_{fs}]$ are the coupling matrices. Relation 1.9 is the starting point for the idea of updating for example the acoustic pressure field based on experimental data related to the vibration of the surrounding structure, allowing to make use of accelerometer based experimental data instead of using microphones to record acoustic pressure fields.

1.2 Acoustic updating technique state of the art

Updating techniques are used when the quality of the numerical model appears to be poor so that the distance with respect to experimental data is above a critical threshold. While updating methods were initially split into two main classes, namely direct and parametric techniques, the distinction is getting looser [MF93]. Parametric techniques need parameterizing the model and resort to an iterative optimization process, as opposed to direct methods. The literature review that follows comes from updating techniques in structural dynamics. Based on chapter 1.1, the presentation of the methods is adapted to the particular domain of acoustics.

1.2.1 Direct updating techniques

Minimum norm methods

Experimental modes are expanded and fill in the columns of the laboratory data matrix, which would be $[\tilde{P}]$ in acoustics. The minimum norm method looks for the symmetric correction matrices $[\Delta M]$ and $[\Delta K]$ (see [Bar82, BN83]) minimizing :

$$\| \, [M]^{1/2} \, [\Delta M] \, [M]^{1/2} \, \|, \tag{1.10}$$

$$\| \, [M]^{1/2} \, [\Delta K] \, [M]^{1/2} \, \|, \tag{1.11}$$

under orthogonality and equilibrium constraints

$$[\tilde{P}]^T [M + \Delta M] [\tilde{P}] = [I], \tag{1.12}$$

$$[\tilde{P}]^T [K + \Delta K] [\tilde{P}] = [\Lambda], \tag{1.13}$$

$$([K + \Delta K] - [\Lambda][M + \Delta M]) \, [\tilde{P}] = 0. \tag{1.14}$$

$[I]$ is the unity matrix, $[\Lambda]$ is the eigenvalue matrix, and $\|.\|$ is the norm of Frobenius, i.e. the sum of the square of all matrix coefficients. Under this form, the technique addresses the correction of both stiffness and mass matrices of undamped systems. The major drawback of the minimum norm method lies in its lack of physics linked to the corrections, even though improvements were brought by some authors.

Matrix mixing methods

Assuming that the whole set of modes of the discrete model is measured, the mass and stiffness matrices of the numerical model are built as follows:

$$[M]^{-1} = [\tilde{P}]^T[\tilde{P}], \tag{1.15}$$

$$[K]^{-1} = [\tilde{P}]^T[\Lambda]^{-1}[\tilde{P}]. \tag{1.16}$$

This method is actually of little use due to the large amount of experimental data to be measured. Authors like [LWB87] and [Cae87] extended the method to make it suitable when unknown modes exist.
Note that the dimensions of the measured eigen vectors have to match the size of the numerical matrices.

Eigenstructure Assignment Method

This is based on the control theory where the input u is linked to the output y via the gain matrix $[G]$ which will determine the corrections to fit the numerical modes and natural frequencies with the experimental data. Assuming that the output can be expressed as a linear combination of the pressure and its first time derivative, the following relation links the input and the output:

$$\{u\} = [G]\{y\} = [G]\left([D_0]\{p\} + [D_1]\{\dot{p}\}\right). \tag{1.17}$$

The system matrix is then written:

$$[K]\{p\} + [C]\{\dot{p}\} + [M]\{\ddot{p}\} - [B_0]\{u\} = 0. \tag{1.18}$$

Then, mixing 1.17 and 1.18 yields

$$\left([K] - [B_0][G][D_0]\right)\{p\} + \left([C] - [B_0][G][D_1]\right)\{\dot{p}\} + [M]\{\ddot{p}\} = 0. \tag{1.19}$$

The main drawbacks of the Eigenstructure Assignment Method lie in the non-unicity of the gain matrix $[G]$ and the non-symmetry of the corrected system matrices, even though some works tend to alleviate those problems (see [IM90, ZW90]).

1.2.2 Parametric updating techniques

The model is assumed to be parameterized. It means that the system matrices are expressed as a function of n parameters x_i, which gives for instance in the case of the correction of the damping matrix :

$$[\Delta C] = \sum_{i=1}^{n} [\Delta C](x_i). \tag{1.20}$$

The updating process consists in finding the parameter set minimizing the cost function $J(\{x\})$ ([Nat88, Tar87]) such that:

$$J(\{x\}) = \|\{R(\{x\})\}\|^2 + \lambda |\{x\} - \{x_0\}|^2. \tag{1.21}$$

The first term in equation 1.21 $\{R(\{x\})\}$ measures the correlation between the discrete model with parameters $\{x\}$ and the laboratory data. $\{R(\{x\})\}$ is called residue or penalization term.
The second term in relation 1.21 is a regularization quantity aiming at favoring a solution $\{x\}$ which is as close as possible to the initial candidate $\{x_0\}$. λ is a parameter to be adjusted which notably allows for weighting differently both contributions in 1.21.

Modal data

The penalization term is written as a combination of the residue on both eigenmodes Φ_i and natural frequencies ω_i. For example, if n eigenmodes are taken into account and the residue is expressed by the Modal Assurance Criterion (MAC), and the chosen norm is a weighted L^2 distance, it yields:

$$\|\{R(\{x\})\}\|^2 = \sum_{i=1}^{n} x_i \left(1 - \mathrm{MAC}\left(\{\tilde{\Phi}\}, \{\Phi\}\right)\right)^2 + \alpha \sum_{i=1}^{n} y_i \left(\frac{\omega_i - \tilde{\omega_i}}{\tilde{\omega_i}}\right)^2. \tag{1.22}$$

α is a weighting factor and the Modal Assurance Criterion is given by:

$$\mathrm{MAC}\left(\{\Phi_i\}, \{\Phi_j\}\right) = \frac{\left(\{\Phi_i\}^T \{\Phi_j\}\right)^2}{\left(\{\Phi_i\}^T \{\Phi_i\}\right)\left(\{\Phi_j\}^T \{\Phi_j\}\right)}. \tag{1.23}$$

Temporal data

Updating methods based on temporal data are only of interest when studying the non linear behavior of a structure. The present study focuses on linear acoustics and will not deal with non linearity occurring in specific domains like aero-acoustics or boundary layer phenomena.

Frequency Response Functions

Those methods are classified by the kind of residue in expression 1.21, which are the input residue, output residue, or constitutive relation error.

Input residue

The input residue postulates that the measured pressure field $\tilde{P}$ is applied to the numerical acoustic model, allowing to compute the resulting force acting on the equivalent model.

$$\left([K] - \omega^2[M] + \mathrm{j}\omega[C]\right)\{\tilde{P}\} = \{F\}. \tag{1.24}$$

At a given frequency ω, the residue is calculated by:

$$\{R(\{x\})\}_\omega = \{F\} - \{\tilde{F}\}. \tag{1.25}$$

Since not all the dof's of the system can be measured, the experimental vector $\{\tilde{F}\}$ is to be expanded based on the numerical information. As a consequence, the measured vector is now depending on the design parameters x_i, and the optimization problem is no more linear. Updating techniques using the input residue are furthermore measurement noise sensitive ([Fri86, CFN84]).

Output residue

The output residue presumes that the numerical model undergoes the force vector that is recorded in the lab. The pressure field is computed using the following equation:

$$\left([K] - \omega^2[M] + \mathrm{j}\omega[C]\right)\{P\} = \{\tilde{F}\}. \tag{1.26}$$

The residue can be calculated at angular frequency ω by:

$$\{R(\{x\})\}_\omega = \{P\} - \{\tilde{P}\}. \tag{1.27}$$

While this optimization problem is also non linear, it appears to be more robust with respect to measurement noise. Those methods are often referred as sensitivity techniques, and the cost function 1.21 is generally approximated by a second order Taylor's development.

Constitutive relation error

The Constitutive Relation Error (CRE) technique is described into details through chapter 2. Other techniques like the Modeling Error in the Constitutive Equations (MECE) ([PGR98]) and the Minimum Dynamic Residual Expansion (MDRE) ([Bal00]) present a formulation of the residue which is pretty close to the one of the CRE.

Chapter 2

Updating 2D acoustic models with the Constitutive Relation Error method [1]

Contents

[1]This chapter is reproduced from: V. Decouvreur, Ph. Bouillard, A. Deraemaeker, and P. Ladevèze. Updating 2D acoustic models with the constitutive relation error, Journal of Sound and Vibration, volume 278(4/5), pages 773-787, 2004.

Nowadays, the increasing importance of the acoustic noise in the industry makes essential to dispose of reliable simulation tools. Furthermore, many industries need to know the acoustic performances of the products that they achieve or use. Indeed, these components are often parts of larger setups (like cars, airplanes, concert halls, theaters,...) for which numerical acoustic simulations are run from the earliest design stage. In that framework, this paper proposes a new updating technique for the acoustic simulations, which is based on the constitutive relation error (CRE) proposed by P. Ladevèze in structural dynamics.
The technique consists in improving the quality of acoustic models by reducing the constitutive relation error below a prescribed level.
The CRE updating method aims at minimizing a cost function with respect to physical parameters of the model. Both modeling error (i.e. the error related to the approximation of physical phenomena) and measurement error are taken into account. Particular attention is paid to the admittance coefficient, which is probably the most important and the most badly known acoustic parameter, and the application to two dimensional finite element numerical simulations is presented showing how promising the technique is.
The ultimate goal of the approach should be to improve the numerical simulations of the acoustic pressure level of real-life complex setups like cars, aircrafts, satellite launchers, etc.

2.1 Introduction

Nowadays, many manufacturing companies have to control the acoustic noise either to improve user's comfort or to decrease environmental pollution. Most of the acoustic simulations are performed using a finite element or a boundary element software.
While computers become faster and faster, allowing decreasing computational time together with smaller calculation error, the acoustic models remain unchanged making the simulations poorly reliable in many cases due to the complexity of the physical phenomena. For instance, the approximative evaluation of the admittance coefficients that are used to run numerical simulations is an example of reason why simulations deviate from experimental data. Indeed, in most of the cases, admittance coefficients are evaluated by achieving experimental measurements on a few samples of a material for which such coefficient is needed. The most classical way to evaluate that coefficient uses a laboratory

setup of Kundt duct type. The admittance coefficient A_n is generally assumed real, what is obviously wrong, since phase shift occurs for waves propagating in porous media. Presently, manufacturers data are limited to the absorption coefficient, what is equivalent to give the modulus of the impedance or admittance coefficient.

In this paper, the idea is to evaluate in situ frequency dependent complex admittance coefficients on the base of a validation stage for a complex incident field. Sound pressure measurements are achieved in a few points of the acoustic domain and admittance coefficients are tuned to verify admittance relations as closely as possible with respect to the physical phenomena.

The values of the admittance coefficients obtained after updating can be used in future numerical simulations. For example, these parameters should be useful in a prototyping phase, when changing the configuration (e.g. the shape of the acoustic domain). The updated values are introduced in the new numerical model of the acoustic domain enabling a good prediction of the acoustic pressure level without having to build a new prototype of the studied setup.

Three different kinds of models are to be considered: the continuous model, the numerical model, and the experimental one. While the continuous and the numerical models are usually the reference and the approximate models respectively, a significant difference appears in the following approach. Indeed, one updates here the continuous model (that is approximated by a numerical model) with respect to experimental data, which constitute the reference.

In what concerns the acoustics, literature treating on updating techniques seems to be poor so that one has to refer to the structural dynamics to get an overview of the existing possibly applicable updating methods. Indeed, the governing equations in dynamics are very similar to those of acoustics; the acoustic pressure and velocities are homologous of the displacement and stresses respectively in structural dynamics. That domain offers more bibliographic sources, leading to distinguish between direct and parametric updating techniques. The direct techniques mainly consist in modifying the mass and stiffness matrices so that numerically simulated and experimentally measured frequency response functions agree as good as possible in terms of natural frequencies. Such modifications lack physical meaning, making the validity domain thin if the configuration changes. In the case of parametric updating techniques, one has to minimize a cost function by tuning physical parameters of the model. The sensitivity of the cost function with respect to the different parameters allows to choose which of these have to be tuned. That choice can also vary with the geometrical localization in the studied domain. A more ex-

tended state of the art on validation methods is presented in [MF93, MKN02]. The present paper proposes to apply a particular parametric updating technique based on the constitutive relation error to the acoustics and to make use of it to get accurate evaluation of complex admittance coefficients. The fundamentals of the CRE were first developed by P. Ladevèze in structural dynamics (see [Lad98, CLP97, DLR04]) and [DBDL02, DBDL04a] introduced the idea of applying the CRE to the acoustics. The main idea in the CRE technique consists in splitting the data and equations of the model into reliable information and less reliable one. Whether one trusts a given data or equation has to be related to the assumptions made to establish that one.
The paper is organized as follows. Firstly, the CRE is applied to the acoustics, and reliable and less reliable data are set. Admissible pressure and velocity fields verifying the reliable equations are built and used to define the CRE. Secondly, we discuss the measurements related error, which leads to consider the modified CRE. Afterwards, the paper deals with a particular numerical approximation of the continuous model, in the circumstances the finite element discretization. Finally, simulations are run on a 2D car cabin to validate the method.

2.2 The CRE applied to the acoustics

2.2.1 Principles

One deals with an acoustic problem that is defined on a domain Ω with boundary $\partial\Omega$. In linear acoustics, one assumes small harmonic perturbations of the particle velocity $\vec{v}$, the pressure p and the density ρ of the isotropic medium so that these oscillations around steady values are respectively written as follows:

$$\begin{cases} \vec{v} = \vec{v}' \mathrm{e}^{\mathrm{j}\omega t} \\ p = p' \mathrm{e}^{\mathrm{j}\omega t} \\ \rho = \rho' \mathrm{e}^{\mathrm{j}\omega t} \end{cases} \tag{2.1}$$

where $\mathrm{j} = \sqrt{-1}$, ω the angular frequency, and t the time.
Let us consider that the reliable equations are the wave equation called Helmholtz equation in the frequency domain and the Dirichlet boundary condition defined on $\partial_1\Omega$ (see figure (2.1) for an illustration of the boundaries):

$$\begin{cases} \text{Helmholtz : } \Delta p + k^2 p = 0 \\ \text{Dirichlet B.C.: } p_{|\partial_1\Omega} = \overline{p} \end{cases} \tag{2.2}$$

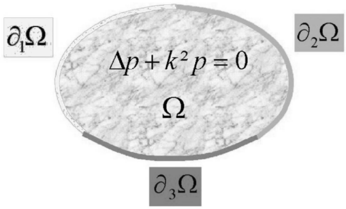

Figure 2.1: studied domain and its boundaries

where c is the sound velocity, and $k = \frac{\omega}{c}$ is the wave number.
The less reliable equations are originally [Lad98] the constitutive relations. Here, we will assume that the mixed Robin boundary condition defined on $\partial_3\Omega$, which links the pressure to the normal velocity by an impedance coefficient Z_n, and the Neumann B.C. defined on $\partial_2\Omega$ are the less reliable data. That latter boundary condition is rewritten in what follows using the Euler equation, which links the pressure gradient to the velocity vector. The resulting two equations are:

$$\begin{cases} \text{Robin B.C.: } v_{n_{|\partial_3\Omega}} = A_n p \\ \text{Neumann B.C.: } v_{n_{|\partial_2\Omega}} = \dfrac{\mathrm{j}}{\omega\rho}\dfrac{\partial p}{\partial n}|_{\partial_2\Omega} = \overline{v}_n \end{cases} \tag{2.3}$$

where $A_n = Z_n^{-1}$ is the complex admittance coefficient, and $\overline{v}_n$ is the prescribed velocity on $\partial_2\Omega$ which is known either by measurement or by structural dynamic computation. Discussions are still open concerning the most appropriate form of admittance relation (2.3). More details can be found in reference [FJT00]. One has chosen here to express the impedance relation under the form:

$$v_n = c_1 p + c_2 \frac{\partial p}{\partial t} \tag{2.4}$$

where c_1 and c_2 are constants and not function of time. Equation (2.4) is equivalent in the frequency domain to:

$$v_n = (c_1 + \mathrm{j}\omega c_2)p = A_n p \tag{2.5}$$

2.2.2 Admissibility

Let us define two Hilbert spaces V_1 and V_2 of functions square-integrable together with their first derivatives in $\overline{\Omega} = \Omega \cup \partial\Omega$:

$$V_1 = H_D^1(\overline{\Omega}) = \{p \in H^1(\overline{\Omega}) | p = \overline{p} \text{ on } \partial_1\Omega\}$$
$$V_2 = H_0^1(\overline{\Omega}) = \{w \in H^1(\overline{\Omega}) | w = 0 \text{ on } \partial_1\Omega\}$$

The variational formulation corresponding to the Helmholtz equation with associated boundary conditions as given in (2.2) and (2.3) is expressed by:

$$\text{Find } p \in V_1 | \int_\Omega (\nabla p \nabla w^* - k^2 p w^*) d\Omega + \mathrm{j}\omega\rho \int_{\partial_3\Omega} v_n w^* d\Gamma$$
$$+\mathrm{j}\omega\rho \int_{\partial_2\Omega} \overline{v}_n w^* d\Gamma = 0 \qquad \forall w \in V_2 \tag{2.6}$$

where * denotes the complex conjugate. The solution $s(p, v_n, \overline{v}_n)$ (where $p, v_n, \overline{v}_n$ are independent fields) $\in \mathbf{S}_{ad}$ (is admissible) if $p \in V_1$ and equation (2.6) is verified.

2.2.3 Definition of the CRE

The CRE is an error which measures the verification of the less reliable equations defined by (2.3). Its value is always positive or equal to zero. It is equal to zero if the Neumann and the Robin equations are verified. The following expression for the CRE will be used :

- error from the Robin B.C.: $\omega^2\rho^2 \int_{\partial_3\Omega} (v_n - A_n p)^* (v_n - A_n p) d\Gamma$

- error from the Neumann B.C.: $\omega^2\rho^2 \int_{\partial_2\Omega} (\overline{v}_n - \frac{\mathrm{j}}{\omega\rho}\frac{\partial p}{\partial n})^* (\overline{v}_n - \frac{\mathrm{j}}{\omega\rho}\frac{\partial p}{\partial n}) d\Gamma$

The CRE ξ_ω^2 measuring the modeling error at angular frequency ω is the sum of the errors related to the poorly reliable relations:

$$
\begin{aligned}
\xi_\omega^2(p, v_n, \overline{v}_n) = {} & \frac{L_2}{L_2+L_3}\gamma\omega^2\rho^2 \int_{\partial_2\Omega} (\overline{v}_n - \frac{\mathrm{j}}{\omega\rho}\frac{\partial p}{\partial n})^* (\overline{v}_n - \frac{\mathrm{j}}{\omega\rho}\frac{\partial p}{\partial n}) d\Gamma \\
& + \frac{L_3}{L_2+L_3}(1-\gamma)\omega^2\rho^2 \int_{\partial_3\Omega} (v_n - A_n p)^* (v_n - A_n p) d\Gamma \qquad (2.7) \\
& \text{where} \left\{ \begin{array}{l} L_2 = \displaystyle\int_{\partial_2\Omega} d\Gamma \\ L_3 = \displaystyle\int_{\partial_3\Omega} d\Gamma \end{array} \right.
\end{aligned}
$$

The factor γ $(0 \leq \gamma \leq 1)$ allows to weight differently the error related to the impedance relation (Robin B.C.) and the one related to the system excitation (Neumann B.C.). The factor γ is to be adjusted by taking into account the a priori knowledge of the studied setup. For example, if the setup excitation is very complex and it is known to be not reliable, the parameter γ should be tuned in function (i.e. γ should tend to one) so that the updating focuses on the error on that B.C. since it is dominant in that case. If no information is available at this subject, γ is set to 0,5.
The interest of using such coefficient is explained by the following example. Let us suppose that the updating process is stopped when reaching a 9% residual CRE level at the end of the validation step (one assumes that 9% is the accuracy level needed for the studied problem). Analyzing the contribution of the error on the Neumann B.C. (ξ_ω^N) and the one on the Robin B.C. (ξ_ω^R) at the end of the optimization shows:

$$\xi_\omega = 0.5 * \xi_\omega^N + 0.5 * \xi_\omega^R = 0.5 * 12\% + 0.5 * 6\% = 9\% \qquad (2.8)$$

The corresponding updated parameters verify the Neumann B.C. with an error of 12% and the Robin B.C. with an error of 6%.
Though, one would prefer to get updated parameters that correspond to an equally distributed error on both B.C. (i.e. something like $\xi_\omega^N \approx \xi_\omega^R \approx 9\%$). Assuming an a priori knowledge of the setup of the type $\xi_\omega^N \approx 2 * \xi_\omega^R$, the coefficient γ is set to 0.75 so that the previously updated parameters that satisfied the CRE threshold now yields:

$$\xi_\omega = \gamma * \xi_\omega^N + (1-\gamma) * \xi_\omega^R = 0.75 * 12\% + 0.25 * 6\% = 10.5\% \qquad (2.9)$$

One can see that using the γ weight forces the updating process to only admit parameters that equally distribute the CRE on both boundary conditions. If no information is available enabling to determine the value of γ before starting the optimization step, the ratio of the errors on the Neumann and Robin B.C. is evaluated at the end of the minimization procedure. It allows to assess the value of the factor γ which is used to run a new optimization process.

2.3 The modified CRE

Since one would like to update a continuous model with reference to experimental measurements, an additional measurement error adds to the error caused by the model formulation itself. Just as for the model, it is necessary to define the reliable and less reliable equations for the measurements and to build an error measure on the less reliable experimental quantities. Measurement errors are among others due to the positioning of the sensors and microphones, their accuracy, calibration, measurement orientation, reproductivity and repeatability of the measurements [Bal98, Bal96, Bal97],...
For instance, measurement errors occur for two types of data:

- pressure measurement by using microphones,
- velocity measurement by using accelerometers or velocity transducers.

2.3.1 The measurement error

In what follows, one assumes that reliable experimental information is:

- the measurement of the angular frequency,
- the positioning of the sensors and microphones,
- the calibration of the sensors and microphones,
- the directions of the measurements and excitations.

These define the admissibility $\mathbf{S}_{ad}$ for the measurements. Considering the two types of measurement error described in section 2.3, the measurement errors at a given frequency are described as follows:

- pressure measurement (amplitude and phase) : $|\Pi_1 p - \Pi_1 \tilde{p}|^2$,

- velocity measurement (amplitude and phase) : $\|\Pi_2\overline{v}_n - \Pi_2\tilde{v}_n\|^2$.

where $\| \quad \|^2$ and $| \quad |^2$ denote energy norms, Π_1 and Π_2 are projection operators that give the value of the pressure and normal velocity respectively at the corresponding sensors, and $\tilde{p}$ and $\tilde{v}_n$ are the measured pressure and normal velocity.
A projection operator Π is a matrix defined by:

$$\begin{cases} \Pi_{ii} = 1 \text{ if the dof } i \text{ is measured} \\ \Pi_{ii} = 0 \text{ if the dof } i \text{ is not measured} \\ \Pi_{ij} = 0 \text{ if } i \neq j \end{cases} \tag{2.10}$$

2.3.2 Quality of a model with respect to measurements: the modified CRE

By summing the constitutive relation error and the measurement error at angular frequency ω, the modified CRE e^2_ω is obtained:

$$e^2_\omega = \xi^2_\omega + \frac{r}{1-r}\{\zeta|\Pi_1 p - \Pi_1\tilde{p}|^2 + (1-\zeta)\|\Pi_2\overline{v}_n - \Pi_2\tilde{v}_n\|^2\} \tag{2.11}$$

where $0 \leq \zeta \leq 1$ and $0 \leq r < 1$. The weighting factor $\frac{r}{1-r}$ translates the trueness in the measurements with respect to the model accuracy. If the error on the measurements is known to be smaller than the modeling error, the parameter r should be consequently adjusted to a value that is lower than 0,5. Indeed, $r = 0,5$ weights equally the modeling error (ξ_ω) and the measurement error.
Similarly, ζ allows to weight the relative importance of the pressure and velocity measurement errors. Indeed, it is assumed that pressure as well as velocity measurements are performed, each of those being polluted. The factor ζ is tuned according to the relative trust that one places in the pressure and velocity measurements. For example, if the pressure measurements are known to be very more polluted than the velocity ones, ζ should tend to 1. Otherwise, ζ is set to 0,5.
The use of these two coefficients r and ζ can be explained in the same way as which has been done for the weight γ.
The modified CRE is an indicator of the verification of the less reliable quan-

tities and equations of the problem. Now the problem becomes :

$$\text{Find } s_\omega(p, v_n, \overline{v}_n) | \quad \begin{cases} s_\omega \in \mathbf{S}_{ad} \\ e^2(s_\omega) \text{ is minimum} \end{cases} \tag{2.12}$$

The solution s_ω will thus verify the reliable equations and quantities exactly by satisfying the admissibility. It will satisfy the less reliable quantities and equations as well as possible by minimizing e^2_ω.
The study of an acoustic system being usually led in a finite frequency range $[\omega_{min}, \omega_{max}]$, a weighting function $z(\omega)$ is defined so that

$$\int_{\omega_{min}}^{\omega_{max}} z(\omega) d\omega = 1 \quad z(\omega) \geq 0 \tag{2.13}$$

and the mean modified CRE in the interval $[\omega_{min}, \omega_{max}]$ is then given by:

$$e^2 = \int_{\omega_{min}}^{\omega_{max}} e^2_\omega z(\omega) d\omega \tag{2.14}$$

If the same weight is attributed to each updating frequency, the function $z(\omega)$ is given by

$$z(\omega) = \frac{1}{\omega_{max} - \omega_{min}} \tag{2.15}$$

More complex functions can be used to focus on a given zone of interest of the frequency range.

2.4 Finite Element discretization

The method proposed in this paper is very general and can be applied to all kinds of numerical approximations like finite element method, boundary element method, meshless method [LBV03], etc. We propose to illustrate here the CRE method in the case of a finite element discretization. It is assumed in what follows that the interpolation and the pollution errors are kept under control by adapting the mesh size to the frequency [DBB99]. Indeed, the sum of these errors has to be sufficiently small compared to the modeling error described before, otherwise the updating presented here does not make sense.

It is first necessary to introduce a pressure formulation by introducing pressure variables (P, Q, R) as follows :

$$p = P \tag{2.16}$$

$$v_n = A_n Q \tag{2.17}$$

$$\overline{v}_n = \frac{\mathrm{j}}{\omega\rho}\frac{\partial R}{\partial n} \tag{2.18}$$

The CRE becomes :

$$\begin{aligned} \xi_\omega^2(P,Q,R) = \gamma\omega^2\rho^2 \int_{\partial_2\Omega} (\frac{\mathrm{j}}{\omega\rho}\frac{\partial P}{\partial n} - \frac{\mathrm{j}}{\omega\rho}\frac{\partial R}{\partial n})^*(\frac{\mathrm{j}}{\omega\rho}\frac{\partial P}{\partial n} - \frac{\mathrm{j}}{\omega\rho}\frac{\partial R}{\partial n})d\Gamma \\ +(1-\gamma)\omega^2\rho^2 \int_{\partial_3\Omega} (A_n P - A_n Q)^*(A_n P - A_n Q)d\Gamma \end{aligned} \tag{2.19}$$

Nodal unknowns are associated to the pressure fields as follows:

Pressure field	Nodal unknown
P	$\mathbf{P}$
Q	$\mathbf{Q}$
R	$\mathbf{R}$

Note that fields Q and R are only defined on $\partial_3\Omega$ and $\partial_2\Omega$ respectively. From the variational formulation (2.6), one writes the corresponding discrete matrix equation:

$$[\mathbf{K}]\mathbf{P} + \mathrm{j}\omega\rho[\mathbf{C}]\mathbf{Q} - \omega^2[\mathbf{M}]\mathbf{P} = [\mathbf{E}]\mathbf{R} \tag{2.20}$$

where

- $p^h = \mathbf{N}^t\mathbf{P}$ is the finite element approximation of the pressure,
- $[\mathbf{M}] = \dfrac{1}{c^2}\displaystyle\int_\Omega \mathbf{N}^t\mathbf{N}d\Omega$ is the mass matrix,
- $[\mathbf{K}] = \displaystyle\int_\Omega \nabla^t\mathbf{N}\nabla\mathbf{N}d\Omega$ is the stiffness matrix,
- $[\mathbf{C}] = \displaystyle\int_{\partial_3\Omega} A_n\mathbf{N}^t\mathbf{N}d\Gamma$ is the impedance matrix,

- $[\mathbf{E}] = \displaystyle\int_{\partial_2\Omega} \nabla_n{}^t\mathbf{N}\mathbf{N}d\Gamma$ is the system excitation matrix due to normal velocities imposed on boundary $\partial_2\Omega$.

CRE (2.7) is written for the FE discretization:

$$\begin{aligned}\xi^2_\omega(\mathbf{P},\mathbf{Q},\mathbf{R}) = \gamma(\mathbf{R}-\mathbf{P})^*[\mathbf{K_n}](\mathbf{R}-\mathbf{P})\\ +(1-\gamma)\rho^2\omega^2(\mathbf{Q}-\mathbf{P})^*[\mathbf{D}](\mathbf{Q}-\mathbf{P})\end{aligned} \tag{2.21}$$

where

- $[\mathbf{K_n}] = \displaystyle\int_{\partial_2\Omega} \nabla_n{}^t\mathbf{N}\nabla_n\mathbf{N}d\Gamma$
- $[\mathbf{D}] = \displaystyle\int_{\partial_3\Omega} A_n^* A_n \mathbf{N}^t\mathbf{N}d\Gamma$

Problem (2.12) to be solved is rewritten:

$$\text{Find } s'_\omega{=}(\mathbf{P},\mathbf{Q},\,\mathbf{R}) \mid \quad \left\{ \begin{array}{l} [\mathbf{K}]\mathbf{P} + \mathrm{j}\omega\rho[\mathbf{C}]\mathbf{Q} - \omega^2[M]\mathbf{P} = [\mathbf{E}]\mathbf{R} \\ e^2_\omega(s') \text{ is minimum} \end{array}\right. \tag{2.22}$$

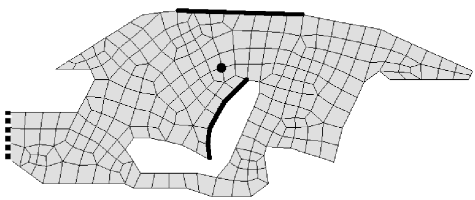

Figure 2.2: 2D mesh of a car cabin

2.5 Two dimensional numerical applications

At this stage, only two dimensional numerical simulations are run. Such problems are of course non realistic (because reality is three dimensional) so that experimental data acquisition is not possible. Consequently, error evaluations are made by comparison with numerical results that are known as being accurate and reliable instead of experimental data.
The updating is performed in a few points located inside the acoustic domain. For the two following studied cases, one limits oneself to the modeling error related to the impedance relation (2.3) and to the pressure measurement error. Pressure measurement is computed at a few points distributed inside the acoustic domain. In practice, it is important to have enough measurement points to be able to filter the noise on these measurements, and to avoid to be in a situation where all measurement points would coincide with pressure nodes, at a given frequency.
There is only one value of $\overline{v}_n$ given on $\partial_2\Omega$, so that the pressure value can be normalized for a unit value of $\overline{v}_n$. In that case, the measurement error is on the pressure only, and the error described in (2.11) reduces to:

$$e_\omega^2 = \omega^2\rho^2 \int_{\partial_3\Omega} (v_n - A_n p)^*(v_n - A_n p)d\Gamma + \frac{r}{1-r}|\Pi_1 p - \Pi_1 \tilde{p}|^2 \tag{2.23}$$

The corresponding relative error for each frequency ω is obtained by dividing e^2 by σ^2, that is for instance:

$$\sigma^2 = \frac{\omega^2\rho^2}{2} \int_{\partial_3\Omega} ((A_n p)^* A_n p + v_n^* v_n)d\Gamma \tag{2.24}$$

The relative modified CRE is then written $e_{rel} = e/\sigma$.

2.5.1 First application: pressure field inside a car cabin with 2 real A_n

Figure (2.2) presents a mesh of the car cabin that has been studied. The mesh comprises 298 nodes and is made up of linear elements with 4 nodes. The excitation of the car structure is caused by the vibration of the firewall. The corresponding boundary condition is represented by a dotted bold line on the mesh. It is assumed in this simulation that only two parts of the cabin are covered by absorbing materials and cause the attenuation of the ambient noise

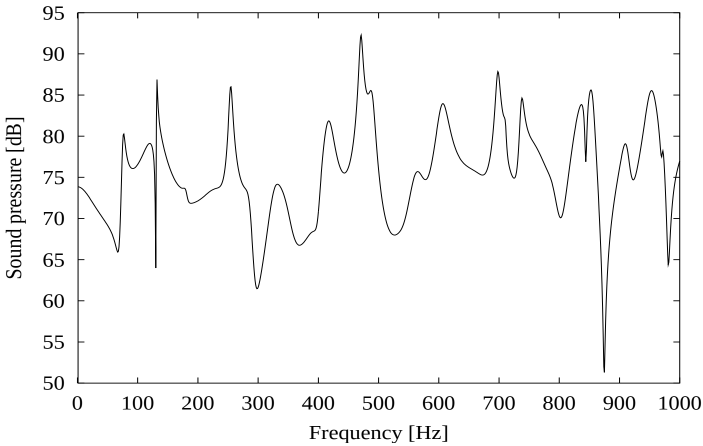

Figure 2.3: Sound pressure FRF at the ear of the driver for mesh (2.2)

inside the car. The first absorbing material overlays a part of the top of the car (see the heavy line in figure (2.2)) with an impedance value $Z_{n1} = 600\text{Nsm}^{-3}$. The second absorbing material corresponds to the front side of the back of the driver seat ($Z_{n2} = 800\text{Nsm}^{-3}$). At this time, impedance values are supposed real for that first application.
The frequency response function of such setup calculated at the ear of the driver (see the bullet on the car mesh (2.2) for the location) is shown in figure (2.3): the frequency range goes from 0 up to 1000 Hz and the ordinate corresponds to the sound pressure FRF in dB when the firewall is excited with a normal velocity equal to 1mms^{-1}. The FRF is computed using the $ACTRAN^{©}$ software developed by Free Field Technologies [Fre02]. The updating algorithm is run for five different frequencies in the range $0-1000$ Hz: $\{20,100,300,600,1000\}$Hz. The updating parameters are the impedances Z_{n1} and Z_{n2} of the absorbing materials described before. Initial values for these unknowns are set to 1000Nsm^{-3}. Figure (2.4) illustrates the modified CRE to be minimized with respect to Z_{n1} and Z_{n2} at each updating frequency. The shown error is frequency averaged and clearly indicates the values of the impedances minimizing the function.
If there are many different admittance coefficients, it is no more possible to

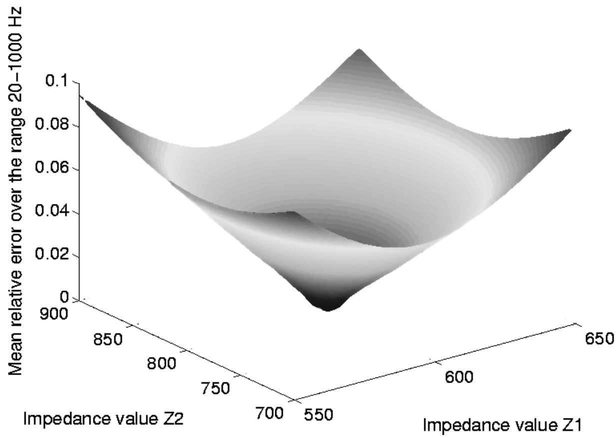

Figure 2.4: frequency averaged modified CRE of the car versus (Z_1, Z_2)

examine the shape of the function to be minimized. That is the reason why the addressed numerical example presents only two admittance coefficients. In the framework of updating models, the unknowns are assumed to be sufficiently close to the initial values that are used at the first iteration of the optimization procedure, so that a local minimization algorithm is used to find the minimum of the error function.
Besides, if one can not guarantee that the global minimum was found, a CRE level after updating that is lower than the one before running the optimization process certifies that the model was improved by the updating procedure.
The optimization algorithm that has been used in the numerical examples is a multidimensional unconstrained nonlinear minimization algorithm of Nelder-Mead [MN65] type.
Running the modified CRE technique implemented in a $MATLAB^{\copyright}$ environment with stopping criterion $e_{rel} \leq 10^{-4}$ yields the two following values for the updated impedances:

$$\begin{cases} Z_{n1} = 600.007 \mathrm{Nsm}^{-3} \\ Z_{n2} = 799.995 \mathrm{Nsm}^{-3} \end{cases}$$

The relative modified CRE for the initial values of the two impedance coefficients Z_{n1} and Z_{n2} was about 38%. After updating the acoustic model, that error diminished below the prescribed value of 0.01%, which shows that the updating technique effectively validates the acoustic model.
For sure, such error level of 0.01% can only be reached for ideal study cases, i.e. without measurement noise and when referring to simulated acoustic fields. Real-life cases should exhibit error values that rarely decay below the 5% barrier.

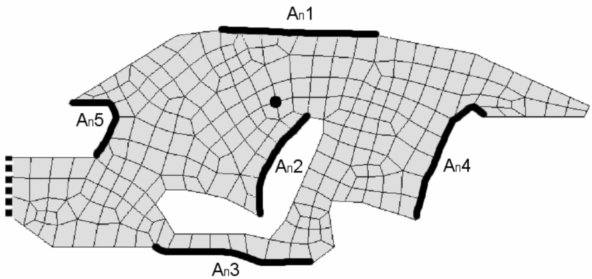

Figure 2.5: 2D mesh of the car cabin with 5 absorbing materials

2.5.2 Second application: updating a 2D car cabin with 5 frequency dependent complex An

The studied setup is the same as before, but the pressure field is now attenuated by the contribution of 5 absorbing materials covering the seats, the roof, the floor and the dashboard of the car. These materials are characterized by complex frequency dependent admittance coefficients of the form: $A_n = C_1 + j\omega C_2$, where C_1 and C_2 are constant values and ω is the angular frequency.
The mesh of the setup is identical to the previous one, but more absorbing materials are now covering the boundaries, as it can be seen on figure (2.5) where the bold lines correspond to the regions covered by one of the absorbing materials.

Unity	$10^{-3}\mathrm{N}^{-1}\mathrm{s}^{-1}\mathrm{m}^{3}$	%
CRE		.05
A_n1	$2 + .002\omega j$	.20
A_n2	$1 - .0015\omega j$	.41
A_n3	$3 + .001\omega j$	.37
A_n4	$5 + .009\omega j$	3.47
A_n5	$4 - .008\omega j$	.77

Table 2.1: Frequency average CRE and error on updated admittance coefficients

Updating without measurement noise

In this application, reference measurements are computed from a FE simulation with the exact values of the 5 updated parameters. Table (2.1) shows the reference values of the admittance coefficients and the error on each of these ones after updating the model from 0 up to 500 Hz. These errors are frequency average values, i.e. each average error is the sum of the errors at each updating frequency divided by the total number of updating frequencies, which is 100 since the setup was updated at each multiple of 5 Hz.
The initial values of the parameters to be updated were set to twice the exact values. Results of table (2.1) are quite satisfying.
Let us note that the number of frequencies at which the setup is to be updated depends on factors like the type of material that is characterized by the updated parameter. Indeed, some materials exhibit high frequency dependence (and thus need lots of updating frequencies) while others present quasi frequency independent behavior.

Updating with measurement noise

In this section, simulated noise is added to the computed measurements. The noise is obtained by multiplying the real and imaginary parts of each measurement by $1 + w * N$, where N is a random number chosen from a normal distribution with mean zero and variance one, and w is the weight applied to the normal distribution, and so the average noise level. The noise affects both the amplitude and the phase of the reference pressure field.
Updating the setup presented above with an average noise level of 5% (i.e.

Unity	$10^{-3}\mathrm{N}^{-1}\mathrm{s}^{-1}\mathrm{m}^{3}$	%
CRE		4.82
A_n1	$2+.002\omega j$	3.39
A_n2	$1-.0015\omega j$	4.55
A_n3	$3+.001\omega j$	2.42
A_n4	$5+.009\omega j$	4.05
A_n5	$4-.008\omega j$	5.08

Table 2.2: Frequency average CRE and error on updated admittance coefficients with measurement noise

$w = 0.05$) generated results of table (2.2). One observes that the error levels after updating are of the order of growth of the average noise level on the measurements.
Figure (2.6) plots the amplitude and the phase of the FRF from 0 up to 500 Hz of the 2D car with the 5 previously defined admittance coefficients. The exact FRF together with the one coming from the updating process with polluted data are plotted. As one can see, the 5% modified CRE level allows for quite a good match with the reference curve.

2.6 Conclusions

A new updating technique inspired from the structural dynamics has been adapted to the acoustics. The goal is here to update a continuous model with reference experimental data.
Based on the constitutive relation error that basically separates data into reliable and less reliable ones, the paper discusses this splitting in what concerns acoustic relations, boundary conditions, and experimental information. Attention is paid to the error coming from experimental measurements that is integrated to the technique which becomes the modified CRE.
The exposed technique applying to every kind of numerical approaches, yet the paper deals with one of these: the finite element formulation. The implemented technique is applied to simulate the sound pressure inside a two dimensional car cabin with absorbing materials on the top and on the driver seat, which constitutes a first validation of the modified CRE technique in acoustics: the impedance values of the absorbing materials are accurately updated. Then, the

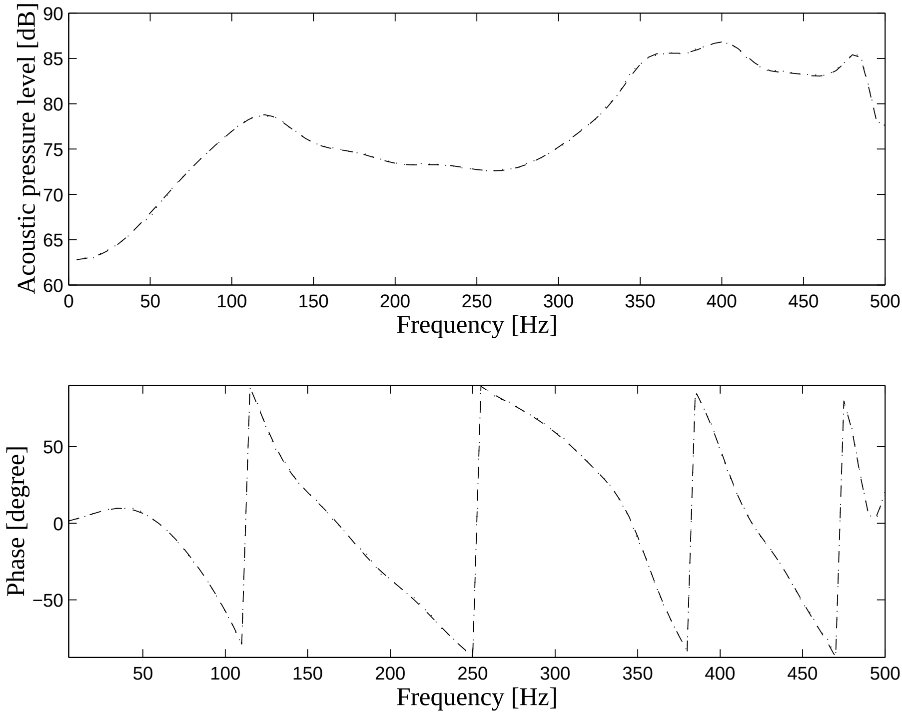

Figure 2.6: Sound pressure FRF at the ear of the driver for 5 A_n with polluted measurements. Dashed line: reference FRF, dotted line: updated FRF

modified CRE updating technique is successfully applied to simulate the sound pressure inside the same car cabin but with 5 absorbing materials defined by frequency dependent complex admittance coefficients covering the boundaries. The same validation is performed when adding simulated noise to the measurements, allowing the technique to still successfully fit the reference FRF with the updated one.
Since the modified CRE updating technique and its application for determining frequency dependent complex admittance coefficients is promising, three dimensional real-life test cases are planned to be achieved, using more realistic models for the admittance coefficient. But model size reduction should precede

the application of the technique presented in this paper to 3D model updating, due to the highly increasing computational time with the number of degrees of freedom, as shown in [DLL02].

Chapter 3

On the effect of the dispersion error when updating acoustic models [1]

Contents

[1] This chapter is reproduced from: V. Decouvreur, E. De Bel, and Ph. Bouillard. On the effect of the dispersion error when updating acoustic models. Comput. Methods Appl. Mech. Engrg., volume 195, pages 394-405, 2006.

In the frame of predicting acoustic pressure fields by means of numerical simulations, many tools are already available, making mostly use of the finite or boundary element techniques.
In order to get simulated acoustic pressure fields closer to the reality, updating techniques can be used. Particularly, one focuses on a validation method based on the Constitutive Law Error (CLE), which was initially proposed by P. Ladevèze [Lad98] in structural dynamics, and was recently applied to acoustics [DBDL04a]. These works use the FEM as numerical approximation method. When increasing the frequency, the validation quality decreases, due to the growing discretization error of the linear FEM.
Therefore, to diminish the discretization error, another approximation method is used, namely the element-free Galerkin method.
A case study is presented where the discretization error is controlled and the effects on the updating parameters (the admittance coefficients) is evaluated. Comparing the results coming from the validation when using both FEM and EFGM shows that a numerical method with robust frequency behavior is more suited for updating setups with highly frequency dependent parameters.

3.1 Introduction

In order to improve the quality of numerical simulations in acoustics, updating techniques based on in situ measurements can be used. The literature dealing with the validation of acoustic models being very light, a review of existing techniques examines corresponding works achieved in structural dynamics. Validation techniques can be split into direct and parametric methods. While direct techniques generally modify the mass and stiffness of the structure to fit the measured natural frequencies, parametric methods modify physical parameters of the model by minimizing a cost function. Whereas the direct updating techniques lack physical meaning, making the validity domain small if the configuration changes, parametric methods improve the knowledge of the model, which can be used again later.
Among the different possible parametric validation techniques, the one based on time data are particularly pertinent when non linear problems are addressed, which is not the case here.
The methods dealing with modal data update the eigen-values and vectors with respect to the parameters. The corresponding experimental eigen-values and vectors have to be measured.

The FRF based techniques can be split into three different classes: the input residue, the output residue and the constitutive law residue techniques. The input residue method consists in applying the measured pressure field to the system to get the corresponding evaluation of the excitation of the acoustic domain. The residue is a function of the difference between that excitation and the measured one. The output residue technique estimates the pressure field computed by exciting the system using the measured excitation vector. The residue is built from the comparison between that pressure field and the measured one.

The latter FRF based method minimizes a residue which is related to the constitutive laws of the system. This paper focuses on the constitutive law error (CLE) proposed by P. Ladevèze in structural dynamics [Lad98]. For instance, recent works applied that technique to validate acoustic models [DBDL02, DBDL04a].

The CLE principles are very general and can be applied to update all kinds of numerical solutions based on the finite element method, boundary element method, etc. Previously, the CLE updating technique was applied to acoustics solved by the finite element method. This analysis was motived by the fact that the FE method is very popular and easy to implement.

The constitutive law that is addressed is the admittance boundary condition, which links the normal velocity to the acoustic pressure by the admittance coefficient. Particularly, we are interested by absorbing materials such as polymeric foams for example. Since these materials are known for their medium and high frequency absorbing behavior, it would be inappropriate to try to record such material characteristics by performing only low frequencies updating simulations.

But it has been shown [DBB99] that for high wave numbers, the Helmholtz equation suffers from the so called dispersion effect: when solving the Helmholtz equation with the classical Galerkin FEM, the accuracy of the numerical solution deteriorates with increasing wave number k. The main effect of the dispersion is that the wave number of the FEM solution is different from the one of the exact solution.

As a consequence, for high wave numbers, the admittance coefficient is wrongly tuned to compensate the dispersion error inherent in the FEM. It leads us to consider an alternative method: the element-free Galerkin method (EFGM). Indeed, [DBB99] and [SB00] have shown the good behavior of this method in terms of dispersion error.

The paper is organized as follows. In section 3.2, the principles of the Con-

stitutive Law Error and its application to acoustics are summarized. Section 3.3 uses the CLE to validate a FE acoustic model of a 2D car cabin whose boundaries are covered by absorbing materials. Then, controlling the dispersion error, its effect on the updating quality is examined showing that the validation results quickly deteriorate with the frequency. Section 3.4 proposes to use an alternative numerical method to achieve the updating, namely the EFGM, whose better behavior with respect to the frequency enables to obtain more accurate results.
Section 3.5 finally compares both approximation methods in terms of CPU-time, showing the interest of using the EFGM to update models with medium wave numbers.

3.2 The CLE applied to the acoustics

3.2.1 Principles

One deals with an acoustic problem defined on a domain Ω with boundary $\partial\Omega$. In linear acoustics, one assumes small harmonic perturbations of the particle velocity $\mathbf{v}$, the pressure p and the density ρ of the isotropic medium so that these oscillations around steady values are respectively written as follows:

$$\begin{cases} \mathbf{v} = \mathbf{v}' e^{j\omega t} \\ p = p' e^{j\omega t} \\ \rho = \rho' e^{j\omega t} \end{cases} \tag{3.1}$$

where $j^2 = -1$, ω is the angular frequency, and t the time.
The pressure field is the solution of the wave equation (called Helmholtz equation in the frequency domain) with associated Dirichlet, Neumann, and mixed Robin boundary conditions on parts $\partial_1\Omega$, $\partial_2\Omega$, and $\partial_3\Omega$ of the frontier respectively. These equations are described in 3.2.

$$\begin{cases} \text{Helmholtz : } \Delta p + k^2 p = 0 \\ \text{Dirichlet B.C.: } p_{|\partial_1\Omega} = \overline{p} \\ \text{Neumann B.C.: } v_{n_{|\partial_2\Omega}} = \dfrac{j}{\omega\rho}\dfrac{\partial p}{\partial n}|_{\partial_2\Omega} = \overline{v}_n \\ \text{mixed Robin B.C.: } v_{n_{|\partial_3\Omega}} = A_n p \end{cases} \tag{3.2}$$

where c is the sound speed, $k = \frac{\omega}{c}$ is the wave number, A_n is the admittance coefficient, and $\overline{v}_n$ is the prescribed velocity exciting the acoustic medium.

Principles of the CLE and its application to acoustics are deeply explained in [DBDL04a]. Here is a short summary of what is necessary to understand the following developments. The idea is to split the available information into reliable and less reliable data. When analyzing the effect of the dispersion error on the updating, it is assumed that the reliable equations are the Helmholtz wave equation in the frequency domain, the Dirichlet boundary condition, and the Neumann B.C. Actually, what is called reliable or less reliable depends on each particular studied case.
The paper deals with the influence of the accuracy of the numerical solution on the quality of the updating. Without loss of generality, the less reliable data considered in the present work is the admittance boundary condition describing the sound absorption in porous media. Different models exist to approximate the wall absorption, but none is completely reliable. The less reliable information yields a residue that is the constitutive law error estimator. Validating a setup then consists in finding the admissible pressure field minimizing the CLE. The tests are performed on purely numerical results by updating the parameters on a coarse grid with respect to the results on a fine grid.

3.2.2 Definition of the CLE

The CLE is an error measuring the satisfaction of the less reliable information. The CLE ξ^2_ω measuring the modeling error at angular frequency ω is given by:

$$\xi^2_\omega(p, v_n) = \omega^2\rho^2 \int_{\partial_3\Omega} (v_n - A_n p)^*(v_n - A_n p)d\Gamma \tag{3.3}$$

where p, v_n are independent fields on $\partial_3\Omega$. The relative error for each frequency ω is obtained by dividing the CLE ξ^2_ω by the following quantity that normalizes the error:

$$\sigma^2_\omega = \frac{\omega^2\rho^2}{2} \int_{\partial_3\Omega} ((A_n p)^* A_n p + v_n^* v_n)d\Gamma \tag{3.4}$$

The relative modified CLE is then written $e^{rel}_\omega = \xi_\omega/\sigma_\omega$.
Approximate pressure variables (P, Q) are defined as follows on $\partial_3\Omega$:

$$p = P \tag{3.5}$$

$$v_n = A_n Q \tag{3.6}$$

A variational formulation of equations 3.2 allows the discretization of the acoustic problem 3.7 where nodal unknowns P, Q are associated to pressure fields $\mathbf{P}$, $\mathbf{Q}$.

$$[K]\mathbf{P} + j\omega\rho[C]\mathbf{Q} - \omega^2[M]\mathbf{P} = [E]\mathbf{P} \tag{3.7}$$

where

- $p^h = \mathbf{N}^t\mathbf{P}$ is the approximate pressure,
- $[M] = \dfrac{1}{c^2}\displaystyle\int_\Omega \mathbf{N}^t\mathbf{N}d\Omega$ is the mass matrix,
- $[K] = \displaystyle\int_\Omega \nabla^t\mathbf{N}\nabla\mathbf{N}d\Omega$ is the stiffness matrix,
- $[C] = \displaystyle\int_{\partial_3\Omega} A_n\mathbf{N}^t\mathbf{N}d\Gamma$ is the admittance matrix,
- $[E] = \displaystyle\int_{\partial_2\Omega} \nabla_n{}^t\mathbf{N}\mathbf{N}d\Gamma$ is the system excitation matrix due to normal velocities prescribed on boundary $\partial_2\Omega$.

The CLE (3.3) is written for the discretized system :

$$\xi^2_\omega(\mathbf{P},\mathbf{Q}) = \rho^2\omega^2(\mathbf{Q}-\mathbf{P})^*[D](\mathbf{Q}-\mathbf{P}) \tag{3.8}$$

where $[D] = \displaystyle\int_{\partial_3\Omega} A_n^* A_n\mathbf{N}^t\mathbf{N}d\Gamma$
The problem to be solved is :

$$\text{Find } s_\omega{=}(\mathbf{P},\mathbf{Q}) \mid \quad \begin{cases} [K]\mathbf{P} + j\omega\rho[C]\mathbf{Q} - \omega^2[M]\mathbf{P} = [E]\mathbf{P} \\ \xi^2_\omega(s_\omega) \text{ is minimum} \end{cases}$$

3.2.3 Less reliable information: the wall admittance

Here, we will assume that the mixed Robin boundary condition which links the pressure to the normal velocity by the admittance coefficient A_n is the less reliable information.
Different models of the admittance coefficient are proposed in the literature.

The choice of the model has to take into account different properties such as the porosity and the thickness of the absorbing material, the stiffness of the skeleton in the case of porous materials, but also the frequency, the incidence angle of the acoustic waves, etc. More detail about admittance models can be found in reference [All93, FJT00].
Again, without less of generality of the proposed approach, this paper focuses on isotropic porous absorbing media with motionless frame and porosity close to 1. These media are represented by an equivalent fluid. The empirical laws of Delany and Bazley describe the wave number inside that fluid together with its characteristic impedance as follows:

$$k_e = \frac{\omega}{c}\left(1 + 0.0978X^{-0.700} - j0.189X^{-0.595}\right) \tag{3.9}$$

$$Z_e = \rho c\left(1 + 0.0571X^{-0.754} - j0.087X^{-0.732}\right) \tag{3.10}$$

where $X = \dfrac{\rho f}{\sigma}$ and $0.01 < X < 1.0$.
$f = \dfrac{\omega}{2\pi}$ is the frequency and σ is the flow resistivity, an intrinsic property of the material that measures the resistance to an air flow through that one. σ lies between 5000 and 100 000 $Nm^{-4}s$ for materials like fiberglass and open-bubble foam.

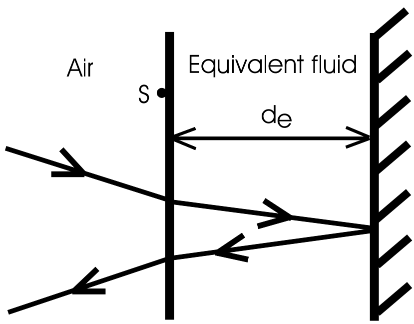

Figure 3.1: Layer of equivalent fluid (thickness d_e) representing an absorbing material backed by a rigid impervious wall

The wall impedance at a point S located on the skin of the absorbing material (see figure 3.1) weakly depends on the angle of incidence so that it can be approximated by:

$$Z(S) = -\frac{jZ_e}{\tan(k_e d_e)} \tag{3.11}$$

3.3 Using the CLE to update a FE model

The aim of this section is to analyze the consequences of the dispersion effect inherent in the FEM on the updating efficiency.

3.3.1 Setup description

The 2D car cabin studied is represented in figure 3.2.
The firewall vibrating with a normal velocity $v_0 = 1mm/s$ excites the acoustic domain. Four regions are covered with different absorbing porous materials represented by hard lines on figure 3.2. The corresponding admittance coefficients are the parameter to be updated. The following parameterized Delany and Bazley model is used for A_n where C_1, C_2, C_3, and C_4 are the coefficients to be tuned:

$$A_n = \left(\rho c\left(1 + C_1 X^{-C_2} - jC_3 X^{-C_4}\right)\right)^{-1} \tag{3.12}$$

Delany and Bazley experiments exhibit values for these coefficients as follows:

$$C_1 = 0.057 \tag{3.13}$$
$$C_2 = 0.754 \tag{3.14}$$
$$C_3 = 0.087 \tag{3.15}$$
$$C_4 = 0.732 \tag{3.16}$$

Each of these absorbing materials is characterized by this model whose coefficients C_1 to C_4 are slightly modified. Initial values for the coefficients are set to 70% of these reference values at the first iteration of each validation process. The flow resistivity σ of the updated porous material is set to $10000Nm^{-4}s$ so that the frequency validity domain is $100Hz < f < 10kHz$ to satisfy $0.01 < X < 1.0$. The thickness of the porous media is set to 10 cm for the seats and 5 cm elsewhere.
The updating is performed in 10 points distributed inside the acoustic domain. A FEA performed on a highly refined mesh is used as a reference solution (p^{ref}) to quantify the discretization error, which is dominated by the dispersion effect

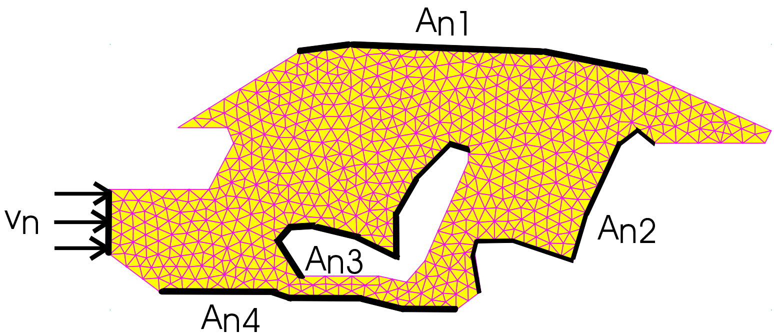

Figure 3.2: 2D mesh of a car cabin with absorbing materials (hard lines)

when increasing the frequency. The discretization error is computed using a L^2 norm:

$$e^2_{disc} = \frac{\int_\Omega \left(p^{ref} - p^h\right)^* \left(p^{ref} - p^h\right) d\Omega}{\int_\Omega p^{ref*} p^{ref} d\Omega} \tag{3.17}$$

The error on A_n is computed by:

$$e^2_{A_n} = \frac{(A_n^{ref} - A_n^{up})^* (A_n^{ref} - A_n^{up})}{A_n^{ref*} A_n^{ref}} \tag{3.18}$$

where A_n^{ref} is the reference exact value of the admittance coefficient and A_n^{up} is the value of A_n obtained by updating the acoustic solution.

3.3.2 Effect of the dispersion error on updating FEM solutions

The validation is performed using the classical linear FEM with 715 nodes and consists in updating the 4 coefficients of the Delany and Bazley admittance model presented in (3.12). Figure 3.3 shows the constitutive law error as a function of kh,where k and h are the wave number and the average mesh size respectively.

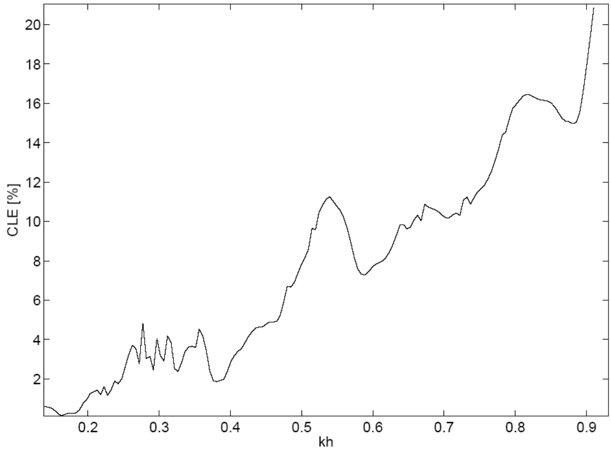

Figure 3.3: CLE vs. kh with 715 dofs using linear FE

If an accuracy of e.g. 5% for the CLE is required when validating an acoustic model, a mesh size satisfying at least $kh = 0.45$ is needed with linear FE (cf. figure 3.3). That is much more demanding than the usual rule of thumb of $kh = 1$ (i.e. six linear elements per wavelength).
Figure 3.4 draws the discretization error together with the error on the updated parameter A_{n1}. Actually, the frequency behavior of the error on the 4 updated admittance coefficients is very similar so that only one of these coefficients is represented in what follows. Figure 3.4 shows the high influence of the dispersion error on the updated parameter A_{n1} that exhibits a high level error when the wave number grows. Indeed, it can be seen on that figure that the updated parameter is wrongly tuned during the validation stage because of the dispersion error.
Figure 3.5 shows pressure fields normalized by the excitation velocity, in dB. The plain curve is the reference computed field (FEA with 32024 nodes). The dotted graph corresponds to the FEM numerical simulation with the exact value of the admittance parameters and 715 nodes, so that the difference between these two curves comes from the dispersion effect.
The dashed FRF on figure 3.5 represents the updated normalized pressure field (FEA with 715 dofs). The validation is not able to correctly tune the parameter

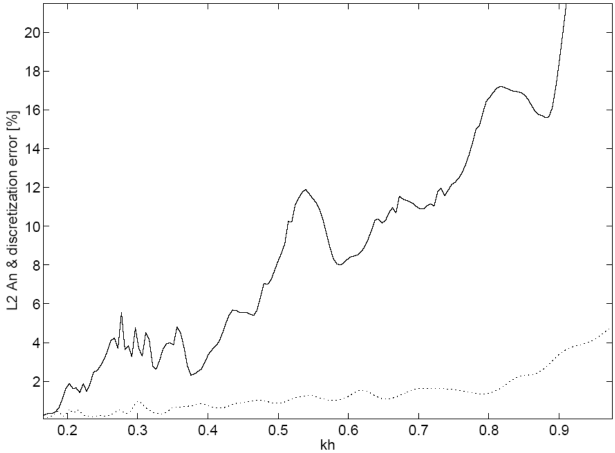

Figure 3.4: A_{n1} error (hard line) and discretization error (dotted line) vs. kh with 715 dofs using linear FE

to fit the exact FRF.
Figures 3.3, 3.4 and 3.5 clearly motive the present study.

3.4 Using the CLE to update an EFG model

Similarly with what has been done in the previous section, the CLE updating technique is now applied to the EFGM (see [LBV03] for detail about applying the EFGM to acoustics). The element-free shape functions are based on the moving least square approximation (MLSA) which is defined on a cloud of nodes. These nodes are not connected by elements. For each node, a domain of influence is defined. In 2-D, that domain is either a disc or a square. The domains are defined to connect the nodes: two nodes are connected if their domains of influence intersect. The influence of a node at a given point is defined by the weight function of that node. The weight function is equal to unity at the node and decreases when the distance to the node increases. The weight function is zero outside the domain of influence of the node. The weight functions that are used for the tests are exponential.

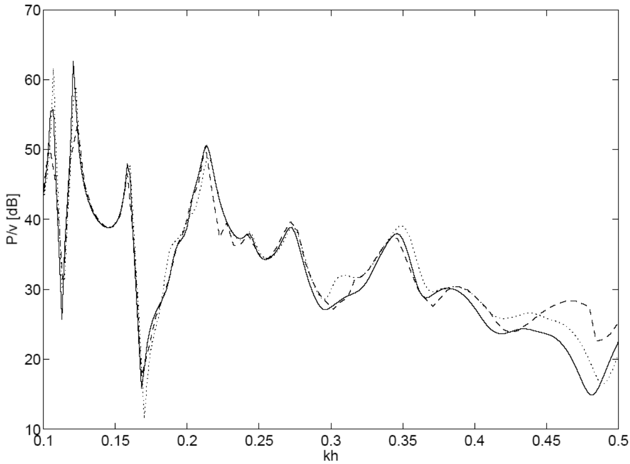

Figure 3.5: Pressure amplitude normalized by the exciting velocity at the driver's ear vs. kh: highly refined FEA reference (32024 nodes, hard line), 715 dofs FE FRF with exact A_{ni} (dotted line), and 715 dofs FE updated FRF (dashed line)

The construction of the MLSA and the corresponding shape functions is based on the choice of a basis $B(x, y)$ of functions that can be polynomial or not.
The EFG approximation used to compute the pressure is of the type (in 2-D):

$$p^h(x, y) = N(x, y)p \tag{3.19}$$

where

$$N(x, y) = B^t(x, y)A(x, y) \tag{3.20}$$

and $A(x, y)$ is a matrix determined by minimizing a L^2 norm.
This formulation furnishes more accurate results compared to the classical linear FEM for 2-D or 3-D acoustics, as shown in [LBV03].
However, precautions have to be taken concerning the particularity of the EFG method which needs to interpolate the nodal pressure values after solving the system (the shape functions are not equal to 1 at the nodes).
Using a trigonometric function basis leads to better results for a given node

distribution at a given frequency. Though, using that latter basis is more expensive in terms of CPU-time, since the shape functions have to be computed at each frequency. To achieve computations on a frequency range and from a CPU-time point of view, the trigonometric function basis is not adapted.
Consequently, a linear basis $B = \{1, x, y\}$ is used for computing the 2-D results in this paper.

3.4.1 Improving the validation quality thanks to the EFGM

In this section, the improvement of the validation quality by making use of the EFGM instead of the FEM as numerical method is shown. Again, the validation aims at finding the appropriate values of the 4 parameters in eq. (3.12).
The comparison of both numerical methods is based on the same nodal distribution, namely 715 nodes like above.
In figure 3.6, the maximum admissible kh leading to a 5% CLE level is plotted

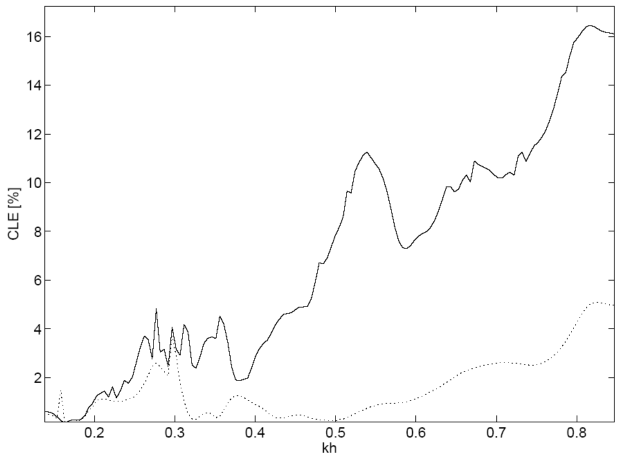

Figure 3.6: CLE of FEM (hard line) and EFGM (dotted line) solutions vs. kh with 715 dofs

for both methods with an average mesh size $h = 0.054$m. The $kh_{max} = 0.75$ of the EFGM is about 1.7 time higher than the one of the FEM.
The corresponding A_{n1} and discretization errors are drawn in figure 3.7.

Finally, figure 3.8 gives the ratio of the pressure field amplitude normalized

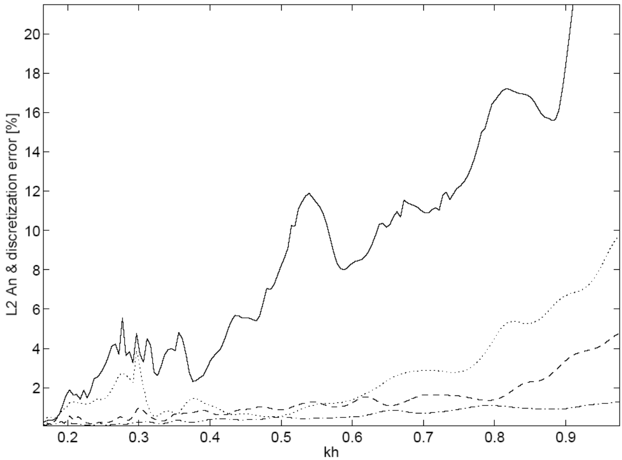

Figure 3.7: Residual errors after updating: FEM A_{n1} error (hard line), FEM dispersion error (dashed line), EFGM A_{n1} error (dotted line), and EFGM dispersion error (dashed dotted line) vs. kh with 715 dofs

by the exciting velocity of the firewall up to $kh = kh_{max}^{EFGM}$.
The solid curve is the reference ratio coming from the FEA with 32024 dofs. The dotted mark corresponds to the ratio coming from the validation of the acoustic problem using the FEM with 715 nodes: for $kh > kh_{max}^{FEM}$, the FEM updated curve clearly differs from the reference. A validation making use of that model at such kh does not make sense.
The dashed line is the updated curve using the EFGM for $kh \leq kh_{max}^{EFGM}$. This line and the reference are nearly merged.

3.5 CPU-time comparison: FEM vs. EFGM to validate models

Whether using the EFGM approximation to update an acoustic model exhibits lower CLE level at a given frequency than the FEM for the same nodal distribution, the CPU-time needed to validate a model with one or the other

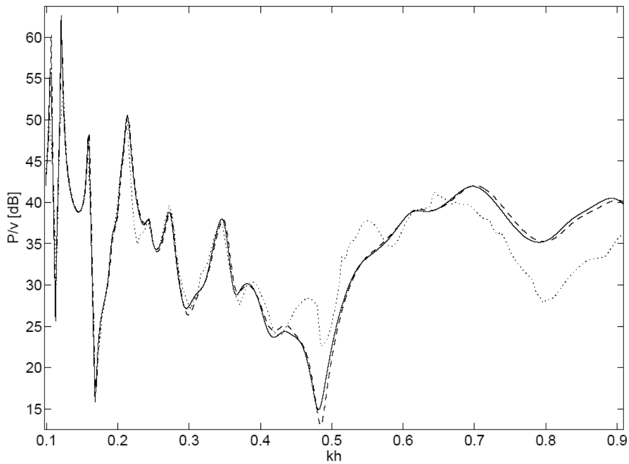

Figure 3.8: Pressure amplitude normalized by the exciting velocity at the driver's ear vs. kh with 715 dofs when validating with FEM (dotted line) and EFGM (dashed line). Continued line: reference ratio (FEA with 32024 nodes)

approximation method is not the same.
Indeed, the EFGM approximation is a little bit more expensive in terms of CPU-time for a same nodal distribution. The reason is that a given node is influenced by more nodes in the EFGM than in the FEM.
Consequently, the EFGM matrices K, M, and C are more crowded than their FEM equivalent, which yields to an increase of the time needed to solve the system.
Now, the question is to know which of both approximation methods is the more efficient.
The answer is given in figure 3.9 where the relative CPU-time is plotted as a function of k_{max} for both approximation methods. The relative CPU-time is the computational time normalized by the running time of the most expensive simulation. Like before, k_{max} is defined as the higher value of k such that the CLE remains below the 5% level for a given node distribution. Each point of the curves on figure 3.9 corresponds to a different discretization.
In order to make the results coming from both approximation methods com-

parable, they are implemented in the same MATLAB© environment, using identical solvers, on the same processors.
Applying the EFGM for validating acoustic models seems to be more efficient than the FEM, already at quite low wave numbers.

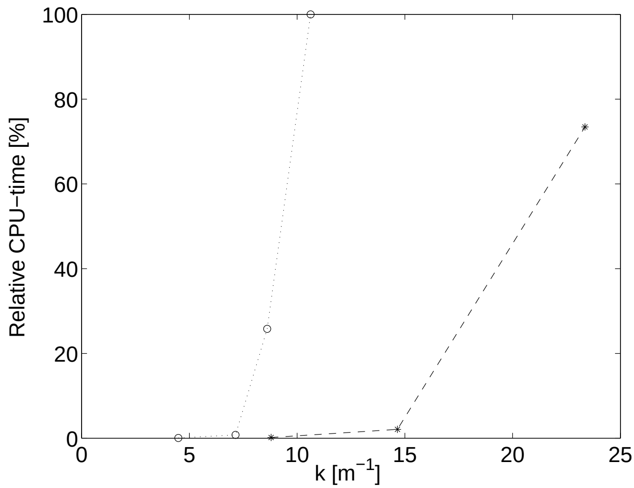

Figure 3.9: k_{max} vs. CPU-time when validating with FEM (dotted line) and EFGM (dashed line)

3.6 Conclusions

Throughout this paper, the important effect of the dispersion error on the results coming from a validation stage is emphasized.
It is shown that validating acoustic models for instance using the CLE is only reliable if the discretization error is very low. For this reason, using the FEM approximation to update acoustic models should only be achieved at low frequencies, unless an extremely refined mesh generating very high computation time is used.
The CLE updating technique appears to be very efficient using the EFGM as an alternative to the FEM when increasing the wave number, since the EFGM

yields to very low CLE level thanks to low dispersion effect at shorter CPU-time compared to the FEM.

Chapter 4

Building a suited reduced modal basis for updating 3D acoustic models with the Constitutive Law Error method [1]

Contents

[1] This chapter is reproduced from: V. Decouvreur, A. Deraemaeker, P. Ladevèze, and Ph. Bouillard. Building a suited reduced modal basis for updating 3D acoustic models with the constitutive law error method, Comput. Methods Appl. Mech. Engrg. 196, pages 3400-3408, 2007.

We have recently reported the possibility of developing an updating technique for acoustic finite element models based on the constitutive law error proposed by P. Ladevèze and co-workers in structural dynamics. Like with every updating technique, we are confronted with and interested in reducing the computational time.
The main idea of this paper consists in building a reduced modal basis made of two contributions: static modes complete a truncated modal basis corresponding to the frequency range of computation. The static modes are associated to the system excitation (for instance a normal velocity boundary condition), but also to the system damping and to the reference measurements.
Updating acoustic models using the reduced modal basis shows a significant CPU-time saving with respect to the full non reduced system with an acceptable accuracy.

4.1 Introduction

In the last years, computer efficiency has increased fast, enabling us to manipulate very large models thanks notably to FEA codes running on a massively parallel architecture. For instance, the Salinas numerical prediction software was developed to run hundreds of millions of degrees of freedom (dofs) problems split among up to tens of thousands of processors with almost linear speedup factors (see [RR00]). These complex heavy models describe generally quite well the geometry and allows us a higher frequency resolution of the problem. Nevertheless, the numerical simulation results are still somewhat too far from the recorded experimental data, which means that the model quality remains unsufficient. A possible solution for improving the model quality makes use of the experimental testing to update the numerical model.
The present paper uses a parametric updating technique based on the constitutive law error (CLE). The fundamentals of the CLE were first developed by P. Ladevèze in structural dynamics (see [Lad98]) and then applied to acoustics in [DBDL04a]. The main idea in the CLE technique consists in splitting the data and equations of the model into 'reliable' information and 'less reliable' one. Whether one trusts a given data or equation has to be related to the assumptions made in its derivation. The choice of the CLE updating technique among the different methods available in the literature is motivated in [DBDL04a].
The updating process is iterative: each step consists in computing new updating parameters and solving the problem using these new values. The computed

pressure is compared to the measurements using the constitutive law error, and the iterative process stops when the error is below a reference threshold value. From a CPU-time point of view, an iterative process is very expensive since the same large model with different parameters has to be computed at each iteration to solve and to update the acoustic problem. From these considerations, large industrial setups can only be updated if the system size is reduced.
In following sections, a reduced basis adapted to the updating of acoustic models with the CLE is formulated, assuming the knowledge of the excitations, the location of measurements, and the possible variations of the updated parameters. The reduced basis is made of a truncated modal basis to which Krylov vectors associated with the excitations are first added. The Krylov subspace technique is well known and largely investigated in the field of structural dynamics ([Bui02]) or circuit simulation ([Fre00]), and references therein. This basis is enriched by static corrections corresponding to forces located at the sensors and to the variable parameters. The building of such a reduced basis is explained and validated on a numerical example. The reason why this reduction technique is chosen among the other possibilities is that the present approach reduces the cost of updating the model drastically. Though, there exist other reduction techniques. For instance, the multimodel approach builds a reduced basis made of truncated modal bases of the model for different values of the parameters (see [Bal96]). The following techniques are quite similar in principles to the one developed here: in [BLC97], the variation of the parameters of the model through the iterations is interpreted as excitations applied to the initial problem. Reduction techniques that are based on sensitivity vectors are other variants of this method (see [Bal98]). Other than using a reduced modal basis, there are alternative techniques, see for example the multipole expansion technique ([Bur94, TA99]).
The paper is organized as follows: after describing the acoustic problem, the CLE principles are shortly summarized. The updating process is explained, together with the discretization of the acoustic problem. The construction of the reduced basis and its application to project the initial problem into a sub-space of lower size enables one to update a numerical example within a significantly lower computation time compared to the updating of the full model.

4.2 The CLE applied to acoustics

4.2.1 Principles

We are dealing with an acoustic problem defined on a domain Ω with boundary $\partial\Omega$. In linear acoustics, one assumes small harmonic perturbations of the particle velocity $\mathbf{v}$, the pressure p and the density ρ of the isotropic medium so that these oscillations around steady values are respectively written as follows:

$$\begin{cases} \mathbf{v} = \mathbf{v}' e^{j\omega t} \\ p = p' e^{j\omega t} \\ \rho = \rho' e^{j\omega t} \end{cases} \tag{4.1}$$

where $j^2 = -1$, ω is the angular frequency, and t the time.
The pressure field is the solution of the wave equation (called Helmholtz equation in the frequency domain) with associated Dirichlet, Neumann, and mixed Robin boundary conditions on parts $\partial_1\Omega$, $\partial_2\Omega$, and $\partial_3\Omega$ of the boundary respectively. These equations are given by (4.2).

$$\begin{cases} \text{Helmholtz}: \ \Delta p + k^2 p = 0 \\ \text{Dirichlet B.C.:} \ p_{|\partial_1\Omega} = \overline{p} \\ \text{Neumann B.C.:} \ v_{n_{|\partial_2\Omega}} = \dfrac{j}{\omega\rho}\dfrac{\partial p}{\partial n}|_{\partial_2\Omega} = \overline{v}_n \\ \text{mixed Robin B.C.:} \ v_{n_{|\partial_3\Omega}} = A_n(\omega) p \end{cases} \tag{4.2}$$

where c is the sound speed, $k = \frac{\omega}{c}$ is the wave number, $A_n(\omega)$ is the admittance coefficient, $\overline{v}_n$ is the prescribed velocity exciting the acoustic medium, and $\overline{p}$ is the imposed pressure on boundary $\partial_1\Omega$. In what follows, the frequency dependence of the admittance coefficients will not be written explicitly and the notation A_n will be used.
Principles of the CLE and its application to acoustics are explained in [DBDL04a]. Here is a short summary of what is necessary to understand the following developments. The idea is to split the available information into reliable and less reliable data. It is assumed that the reliable equations are the Helmholtz wave equation in the frequency domain, the Dirichlet boundary condition, and the Neumann boundary condition. It has to be noticed though, that what is called reliable or less reliable depends on each application.
The less reliable data considered in the present work is the admittance boundary condition describing the sound absorption in porous media. Indeed, different models exist to approximate the wall absorption, but none is completely

reliable. The less reliable information yields a residue that is the constitutive law error estimator. Updating a setup then consists in finding the admissible pressure field minimizing the CLE.

4.2.2 Definition of the CLE

The CLE is an error measuring the satisfaction of the less reliable information. The CLE ξ_ω^2 measuring the modeling error at angular frequency ω is given here by:

$$\xi_\omega^2(p, v_n) = \omega^2 \rho^2 \int_{\partial_3 \Omega} (v_n - A_n p)^* (v_n - A_n p) d\Gamma \tag{4.3}$$

where p, v_n are independent fields on $\partial_3 \Omega$. The relative error for each frequency ω is obtained by dividing the CLE ξ_ω^2 by the following quantity that normalizes the error:

$$\sigma_\omega^2 = \frac{\omega^2 \rho^2}{2} \int_{\partial_3 \Omega} ((A_n p)^* A_n p + v_n^* v_n) d\Gamma \tag{4.4}$$

The relative modified CLE is then written $e_\omega^{rel} = \xi_\omega / \sigma_\omega$.

4.2.3 The modified CLE

Since we want to update a continuous model with reference to experimental measurements, an additional measurement error is added to the error ξ_ω caused by the model formulation itself. Just as for the model, it is useful to define the reliable and less reliable equations for the measurements and to build an error measure on the less reliable experimental quantities. Measurement errors are among others due to the positioning of the sensors and microphones, their accuracy, calibration, measurement orientation,...
If we are dealing with pressure measurement by using microphones and we assume that only the measured amplitudes are less reliable, then the relative modified CLE is written:

$$e_\omega^{rel} \quad = \quad \left(\frac{\xi_\omega^2}{\sigma_\omega^2} + \frac{r}{1-r} \frac{\|\Pi p - \tilde{p}\|^2}{\|\tilde{p}\|^2} \right)^{1/2} \tag{4.5}$$

4.2.4 Discrete updating problem

Approximated pressure variables (P, Q) are defined as follows on $\partial_3\Omega$:

$$p = P \tag{4.6}$$
$$v_n = A_n Q \tag{4.7}$$

A variational formulation of equations (4.2) allows the discretization of the acoustic problem where nodal unknowns $\mathbf{P}$, $\mathbf{Q}$ are associated to pressure fields P, Q.

$$[\mathbf{K}]\mathbf{P} + j\omega\rho[\mathbf{C}]\mathbf{Q} - \omega^2[\mathbf{M}]\mathbf{P} = [\mathbf{E}]\mathbf{P} \tag{4.8}$$

where

- $p^h = \mathbf{N}^t\mathbf{P}$ is the approximate pressure,
- $[\mathbf{M}] = \frac{1}{c^2}\int_\Omega \mathbf{N}^t\mathbf{N}d\Omega$ is the mass matrix,
- $[\mathbf{K}] = \int_\Omega \nabla^t\mathbf{N}\nabla\mathbf{N}d\Omega$ is the 'stiffness' matrix,
- $[\mathbf{C}] = \int_{\partial_3\Omega} A_n\mathbf{N}^t\mathbf{N}d\Gamma$ is the admittance matrix,
- $[\mathbf{E}] = \int_{\partial_2\Omega} \nabla_n{}^t\mathbf{N}\mathbf{N}d\Gamma$ is the system excitation matrix due to normal velocities prescribed on boundary $\partial_2\Omega$.

The modeling CLE (4.3) is written for the discretized system :

$$\xi^2_\omega(\mathbf{P},\mathbf{Q}) = \rho^2\omega^2(\mathbf{Q}-\mathbf{P})^*[\mathbf{D}](\mathbf{Q}-\mathbf{P}) \tag{4.9}$$

where $[\mathbf{D}] = \int_{\partial_3\Omega} A_n^* A_n\mathbf{N}^t\mathbf{N}d\Gamma$
The discrete form of the modified CLE (4.5) taking into account the experimental error is given by:

$$e^2_\omega = \xi^2_\omega + \frac{r}{1-r}\{\mathbf{\Pi P} - \tilde{\mathbf{P}}\}^*[\mathbf{G_w}]\{\mathbf{\Pi P} - \tilde{\mathbf{P}}\} \tag{4.10}$$

where $[G_w]$ represents the error measure $\|.\|^2$, Π is a projection operator that gives the value of the pressure at the corresponding sensors, $\tilde{p}$ is the measured pressure, and $\tilde{\mathbf{P}}$ the corresponding nodal value vector.
A projection operator $\mathbf{\Pi}$ is a matrix defined by:

$$\begin{cases} \Pi_{ii} = 1 \text{ if the dof } i \text{ is measured} \\ \Pi_{ii} = 0 \text{ if the dof } i \text{ is not measured} \\ \Pi_{ij} = 0 \text{ if } i \neq j \end{cases} \tag{4.11}$$

In the numerical example of this paper, $[\mathbf{G_w}]$ is a square unity matrix of size equal to the number of measurements. The weighting factor $\frac{r}{1-r}$ is related to the trust that we put in the measurements with respect to the model accuracy. Reference [DLR04] shows that for usual noise level on the experimental data and modeling error, $r = 0.5$ is a good choice.
The problem to be solved is :

$$\text{Find } s_\omega{=}(\mathbf{P},\mathbf{Q}) \mid \begin{cases} [\mathbf{K}]\mathbf{P} + j\omega\rho[\mathbf{C}]\mathbf{Q} - \omega^2[\mathbf{M}]\mathbf{P} = [\mathbf{E}]\mathbf{P} \\ \xi^2_\omega(s_\omega) \text{ is minimum} \end{cases} \tag{4.12}$$

The updating process consists in solving problem (4.12), which is done iteratively. At each iteration, the functional e^2_ω (4.10) is evaluated and compared to a required quality level e^2_0 until $e^2_\omega \leq e^2_0$.

4.3 Model reduction

The minimization of e^2_ω under the admissibility constraint is achieved here by introducing Lagrange multipliers, which leads to equation (4.13).

$$\frac{1}{2}(\mathbf{Q}-\mathbf{P})^*[\mathbf{C}](\mathbf{Q}-\mathbf{P}) + \frac{r}{2(1-r)}(\mathbf{\Pi P}-\tilde{\mathbf{P}})^*[\mathbf{G_w}](\mathbf{\Pi P}-\tilde{\mathbf{P}}) \\ + \mathbf{\Lambda}^*\left\{([\mathbf{K}]-\omega^2[\mathbf{M}])\mathbf{P} + j\omega\rho[\mathbf{C}]\mathbf{Q} - [\mathbf{E}]\mathbf{P}\right\} \tag{4.13}$$

Problem (4.12) is solved by deriving equation (4.13) with respect to $\mathbf{P}$, $\mathbf{Q}$, and the Lagrange multiplier $\mathbf{\Lambda}$.
By eliminating the Lagrange multiplier, the previous system can be rewritten under the form of two undamped forced vibration problems, the first in $\mathbf{P}$ and the second in $(\mathbf{Q}-\mathbf{P})$:

$$([\mathbf{K}]-\omega^{\mathbf{2}}[\mathbf{M}])\mathbf{P} = \mathbf{b} - j\omega\rho[\mathbf{C}]\mathbf{Q} \tag{4.14}$$

$$([\mathbf{K}]-\omega^{\mathbf{2}}[\mathbf{M}])(\mathbf{Q}-\mathbf{P}) = j\omega\rho[\mathbf{C}](\mathbf{Q}-\mathbf{P}) + j\frac{\omega r}{1-r}\mathbf{\Pi}^t[\mathbf{G_w}](\tilde{\mathbf{P}}-\mathbf{\Pi P}) \tag{4.15}$$

where $\mathbf{b} = [\mathbf{E}]\mathbf{P}$. Such problems can be reduced using a truncated modal basis to which Krylov vectors associated to the force-like terms in the right hand side are added. This technique is inspired from paper [DLL02], that suggested the idea in the case of the structural dynamics.

4.3.1 Truncated modal basis

Let us consider the following classical undamped forced vibration problem at angular frequency ω, in its discrete form:

$$([\mathbf{K}] - \omega^{\mathbf{2}}[\mathbf{M}])\mathbf{P} = \mathbf{F} \tag{4.16}$$

For a system with N degrees of freedom, there are N pairs $(\mathbf{\Phi_i}, \omega_i)$ that verify:

$$([\mathbf{K}] - \omega_{\mathbf{i}}^{\mathbf{2}}[\mathbf{M}])\mathbf{\Phi_i} = \mathbf{0} \tag{4.17}$$

A truncated model basis is built by taking L eigenmodes such that for $i > L$, $\omega/\omega_i \ll 1$.
The approximation can be improved by adding to the truncated modal basis series of Krylov vectors associated with the excitation $\mathbf{F}$. The series are defined as follows:

$$[\mathbf{K}]^{-\mathbf{1}} \left([\mathbf{M}][\mathbf{K}]^{-\mathbf{1}}\right)^{\mathbf{k}} \mathbf{F}, \quad k = 0, 1, 2, \ldots \tag{4.18}$$

More details about Krylov series can be found in [Qu01]. The first term of the series is the static response of the system to the excitation $\mathbf{F}$, while the next terms represent static responses to the forces $\left([\mathbf{M}][\mathbf{K}]^{-\mathbf{1}}\right)^{\mathbf{k}} \mathbf{F}$.

4.3.2 Application to the reduction of problem (4.12)

Excitations in equations (4.14) and (4.15)

The right hand side of equation (4.14) can be split into two different contributions:

- $\mathbf{b}$ (excitation applied to the system) $= \mathbf{F_1}$
- $-j\omega\rho[\mathbf{C}]\mathbf{Q} = \mathbf{F_2}$

The right hand side of equation (4.15) shows also two contributions:

- $j\omega\rho[\mathbf{C}](\mathbf{Q} - \mathbf{P}) = \mathbf{F_3}$
- $j\omega\frac{r}{1-r}\mathbf{\Pi^t}[\mathbf{G_w}](\tilde{\mathbf{P}} - \mathbf{\Pi P}) = \mathbf{F_4}$

Approximation of the excitations

Among the excitations F_1 to F_4, only $F_1 = \mathbf{b}$ is known. The other forces are approximated in what follows. The components of $\mathbf{F_4}$ are zero except for the measured degrees of freedom. This force can be considered as the sum of unit forces $\mathbf{F_{4,i}}$ at each of the sensors:

$$\mathbf{F_4} = \sum_{i=1}^{NS} a_i \mathbf{F_{4,i}} \tag{4.19}$$

where NS is the number of sensors.
The vector $\mathbf{F_2}$ is a function of $\mathbf{Q}$, which can be approximated by:

$$\begin{aligned} \mathbf{Q} &= [\mathbf{T_0}]\mathbf{Q_r} && (4.20) \\ \text{with } [\mathbf{T_0}] &= [\mathbf{\Phi_1} \quad \dots \quad \mathbf{\Phi_L} \quad [\mathbf{K}]^{-\mathbf{1}}\mathbf{F_{4,i}} \quad \dots \quad [\mathbf{K}]^{-\mathbf{1}}\mathbf{F_{4,NS}}] && (4.21) \end{aligned}$$

Neglecting the $[\mathbf{K}]^{-\mathbf{1}}\mathbf{F_{4,i}}$ basis vectors that are a correction to the truncated modal basis $[\mathbf{\Phi}]$, $\mathbf{F_2}$ can thus be approximated by:

$$\mathbf{F_2} = \sum_{i=1}^{L} a_i [\mathbf{C}]\mathbf{\Phi_i} \tag{4.22}$$

This approach is similar to what is done in [BLC97], [Bal98] and [BB01].
Similarly with what has been done to approximate $\mathbf{F_2}$, the vector $\mathbf{F_3}$ can be expressed as:

$$\mathbf{F_3} = \sum_{i=1}^{L} b_i [\mathbf{C}]\mathbf{\Phi_i} \tag{4.23}$$

Since the forces $\mathbf{F_2}$ and $\mathbf{F_3}$ are made of the same basis vectors (only the multiplying coefficients are different), only one of these forces has to be considered concerning its contribution in terms of the basis vectors needed to build the reduced basis.

Damping matrix modification during the optimization process

During the optimization process, the damping matrix $[\mathbf{C}]$ is modified at each iteration and becomes $[\mathbf{C} + \mathbf{\Delta C}]$. The forced vibration problems are consequently modified by adding a term of the form $\mathbf{F_c} = [\mathbf{\Delta C}]\mathbf{P}$ on the right hand side. Using the same approach as in section 4.3.2, $\mathbf{F_c}$ is approximated by:

$$\mathbf{F_c} = \sum_{i=1}^{L} c_i[\mathbf{\Delta C}]\mathbf{\Phi_i} \tag{4.24}$$

The Robin boundary condition can be subdivided in H regions that correspond to the different absorbing material regions. Each region is characterized by an admittance coefficient $A_{n,j}$ and an admittance matrix $[\mathbf{C_j}]$ whose coefficients are zero at the nodes outside this region so that:

$$[\mathbf{C}] = \sum_{j=1}^{H} A_{n,j}[\mathbf{C_j}] \tag{4.25}$$

It will now be shown that the modified damping matrices $[\mathbf{\Delta C_j}]$ ($j = 1, \ldots, H$) are proportional to the local matrices $[\mathbf{C_j}]$.
If $[.]^k$ denotes the iteration number k, equation (4.25) becomes:

$$[\mathbf{C}]^k \quad = \quad \sum_{j=1}^{H} A_{n,j}^k[\mathbf{C_j}] \tag{4.26}$$

Defining the damping matrix modification at iteration k by

$$[\mathbf{\Delta C}]^k = [\mathbf{C}]^{\mathbf{k}} - [\mathbf{C}]^{\mathbf{0}} \tag{4.27}$$

combining (4.26) and (4.27) gives

$$\begin{aligned}
[\mathbf{\Delta C}]^k &= \sum_{j=1}^{H}(A_{n,j}^k[\mathbf{C_j}] - \sum_{j=1}^{H}(A_{n,j}^0[\mathbf{C_j}] && (4.28)\\
&= \sum_{j=1}^{H}(A_{n,j}^k - A_{n,j}^0)[\mathbf{C_j}] && (4.29)\\
&= \sum_{j=1}^{H}[\mathbf{\Delta C_j}]^k && (4.30)
\end{aligned}$$

Comparing the last two lines clearly shows that $[\mathbf{\Delta C_j}]^k$ is proportional to $[\mathbf{C_j}]$, which yields:

$$\mathbf{F_c} = \sum_{i=1}^{L} c_i[\mathbf{\Delta C}]\mathbf{\Phi_i} \tag{4.31}$$

$$= \sum_{i=1}^{L}\sum_{j=1}^{H} c_{ij}[\mathbf{C_j}]\mathbf{\Phi_i} \tag{4.32}$$

Model projection in the reduced space

The contributions to the excitation of the undamped vibration problems leads to build a static basis $\mathbf{T_{stat}}$. If only the first term of the Krylov series is kept, the forces $\mathbf{F_i}$ $(i = 1, \ldots, 4)$ and $\mathbf{F_c}$ yield the corresponding static basis contributions, that are expressed as follows:

$$\mathbf{F_1} \dashrightarrow \mathbf{T_{stat,1}} = \left[[\mathbf{K}]^{-1}\mathbf{F_1}\right] \tag{4.33}$$

$$\mathbf{F_2}, \mathbf{F_3} \dashrightarrow \mathbf{T_{stat,2}} = \left[[\mathbf{K}]^{-1}[\mathbf{C}]\mathbf{\Phi_1} \quad \ldots \quad [\mathbf{K}]^{-1}[\mathbf{C}]\mathbf{\Phi_L}\right] \tag{4.34}$$

$$\mathbf{F_4} \dashrightarrow \mathbf{T_{stat,4}} = \left[[\mathbf{K}]^{-1}\mathbf{F_{4,1}} \quad \ldots \quad [\mathbf{K}]^{-1}\mathbf{F_{4,NS}}\right] \tag{4.35}$$

$$\mathbf{F_C} \dashrightarrow \mathbf{T_{stat,c}} = \left[[\mathbf{K}]^{-1}[\mathbf{C_1}]\mathbf{\Phi_1} \quad \ldots \quad [\mathbf{K}]^{-1}[\mathbf{C_1}]\mathbf{\Phi_L}\right. \tag{4.36}$$

$$\left.\ldots \quad [\mathbf{K}]^{-1}[\mathbf{C_H}]\mathbf{\Phi_1} \quad \ldots \quad [\mathbf{K}]^{-1}[\mathbf{C_H}]\mathbf{\Phi_L}\right] \tag{4.37}$$

Finally, the static basis $\mathbf{T_{stat,2}}$ is left out because its vectors are linear combinations of the basis vectors of $\mathbf{T_{stat,c}}$. The final reduced basis for the updating system is :

$$[\mathbf{T}] = [\quad [\mathbf{\Phi}] \quad [\mathbf{T_{stat,1}}] \quad [\mathbf{T_{stat,4}}] \quad [\mathbf{T_{stat,c}}] \quad] \tag{4.38}$$

The reduced quantities can now be expressed as follows:

$$\mathbf{P} = [\mathbf{T}]\mathbf{P_r} \tag{4.39}$$

$$\mathbf{Q} - \mathbf{P} = [\mathbf{T}](\mathbf{Q} - \mathbf{P})_\mathbf{r} \tag{4.40}$$

$$\mathbf{b_r} = [\mathbf{T}]^\mathbf{t}\mathbf{b} \tag{4.41}$$

$$[\mathbf{K_r}] = [\mathbf{T}]^\mathbf{t}[\mathbf{K}][\mathbf{T}] \tag{4.42}$$

$$[\mathbf{M_r}] = [\mathbf{T}]^\mathbf{t}[\mathbf{M}][\mathbf{T}] \tag{4.43}$$

$$[\mathbf{C_r}] = [\mathbf{T}]^\mathbf{t}[\mathbf{C}][\mathbf{T}] \tag{4.44}$$

$$[\mathbf{\Pi_r}] = [\mathbf{\Pi}][\mathbf{T}] \tag{4.45}$$

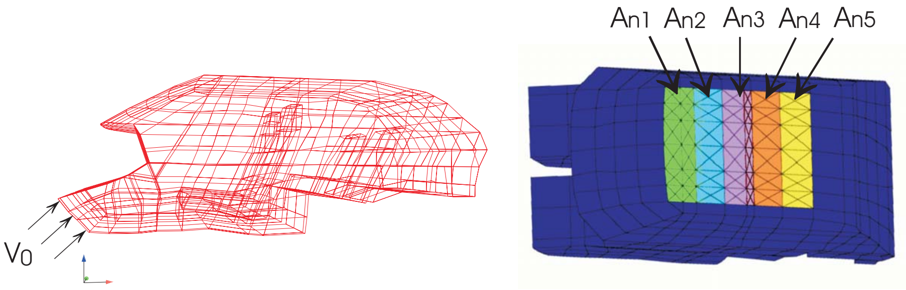

Figure 4.1: Side and top view of the mesh of the light model of a car cabin

Note that the basis is orthonormalized to improve the system conditioning. Note also that the reduced basis is built from undamped eigenmodes. Consequently, that basis could only be used to represent the behavior of a slightly damped system, assuming that its eigenmodes are close the one of the corresponding undamped system.

4.4 Numerical applications

Two applications of the technique are proposed in this section. The first test-case addresses a light model. The objective is to validate the technique feasibility and check the ability of the different contributions of the reduced basis to improve the quality of the updated results.
The second numerical application deals with a 20.000 node mesh for which projecting the initial model into a sub-space is of real interest. A detailed analysis of the updated parameters is performed along the studied frequency range.

4.4.1 Validation of the reduced basis on a light model

The studied setup is a simplified model of a 3D car cabin that is presented in figure (4.1). The finite element mesh contents 1171 nodes and 814 linear elements (69 wedges and 745 bricks), and it is excited by its firewall that vibrates with normal velocity $v_0 = 1mm/s$.

64.3	137.4	183.9	221.4	261.3	280.8
107.9	151.1	189.9	244.8	269.0	286.7
118.9	158.7	217.5	260.1	277.2	294.5

Table 4.1: Eigenfrequencies of the light acoustic model (fig.4.1) in the range [0-300] Hz

The roof of the car is covered by 5 different absorbing materials with admittance coefficients $A_{n1}, A_{n2}, A_{n3}, A_{n4}, A_{n5}$. These parameters are complex and frequency dependent and the goal is to update them by minimizing the CLE. The remaining bounding surface of the car body is assumed to be rigid.
Measurements were not performed and the reference pressure field that is used to validate the model comes from a finite element simulation with the exact value of the 5 unknown parameters. A total of 16 nodal pressures simulating as many sensors located near the absorbing materials are taken into account. The validation of the model is achieved in the frequency range $[0-150]$ Hz with a frequency step of 2 Hz. The natural frequencies in the range $[0-300]$ Hz are presented in table (4.1). The initial values of the 5 admittance coefficients at the first iteration of the optimization process are set to the double of their exact values. The validation step is run using different reduced bases.
The results are reported in table (4.2), showing the residual CLE after validating the setup (column 2), the residual error on the 5 updated parameters, the size of the basis used (number of vectors in the basis) and the CPU-time needed to update the setup on the studied frequency range. The error levels (in %)

Basis #	CLE [%]	A_{n1} error [%]	A_{n2} error [%]	A_{n3} error [%]	A_{n4} error [%]	A_{n5} error [%]	size(T)	CPU-time [minutes]
1	19.1	/	/	/	/	/	18	50
2	0.49	1.31	5.40	2.03	1.25	4.34	64	94
3	0.07	0.56	2.76	0.88	0.39	0.77	78	127

Table 4.2: Residual CLE after validating the setup (column 2), residual error on the 5 updated parameters, size of the basis used (number of vectors in the basis) and CPU-time needed to update the setup

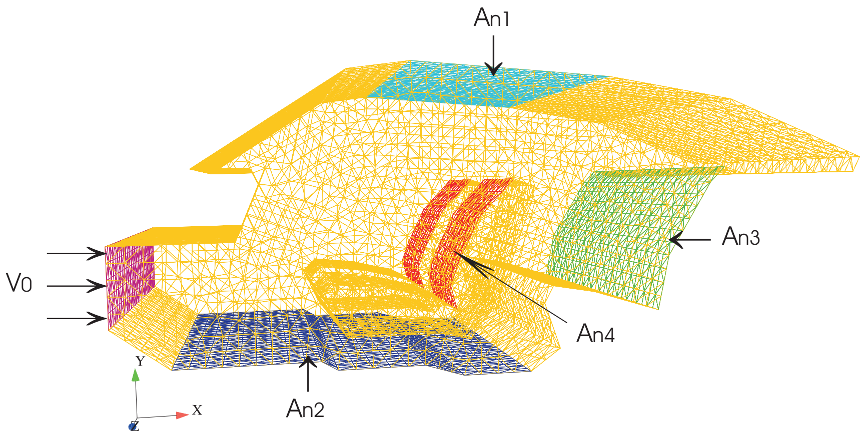

Figure 4.2: Side view of the car cabin mesh and its boundary conditions

are frequency average values. The error values on the admittance coefficients for the basis 1 explode and are therefore not mentioned.
The description of the 3 reduced bases is the following one:

- basis 1: eigenmodes in the frequency range [0-300] Hz,
- basis 2: basis 1 + $\mathbf{T_{stat,1}}$ + $\mathbf{T_{stat,c}}$,
- basis 3: basis 2 + $\mathbf{T_{stat,4}}$

Table (4.2) shows that a classical truncated modal basis (basis 1) is unable to simulate the behavior of the setup. Adding the static response of the system to the excitation $\mathbf{b}$ and taking into account the forces related to the system variations (basis 2) improves significantly the CLE threshold, but very low error levels on the updated parameters can only be reached by adding static responses linked to the unity vectors associated to the measured degrees of freedom (basis 3).
Finally, the residual error levels on the admittance coefficients and the CLE are very low (mostly less than 1%), which is comparable to the stop criterion e_0

that is used when updating the acoustic problem with the full discrete system. So, the updating quality with the reduced basis is like the one of the full system, which validates the reduced basis.

4.4.2 Acoustic absorption in a car cabin

This numerical application is intended to apply the constitutive law error updating technique while using the reduced basis developed trough chapter 4.3 to a model with a mesh density justifying the need for the model size reduction. The geometry is pretty similar to the one of the first numerical example in the sense that it represents also the acoustic domain of a car cabin. The outer shape of the setup is nevertheless somewhat different (in this case the trunk is not represented for instance) and the seat sketching was improved. The longitudinal length of the present device is also somewhat shorter, which explains why the eigenfrequencies are typically higher.
The mesh is made of 19.725 nodes and 100.087 linear tetrahedral elements. One focuses on the acoustic absorption related to the materials covering the roof, the floor and the back-rest of both the front and the rear seats of the car. Admittance coefficients correspondence is the following one:

- A_{n1} refers to the roof of the car as represented in fig.(4.2),
- A_{n2} refers to the floor of the car,
- A_{n3} refers to the back-rest of the rear seat of the car,
- A_{n4} refers to the back-rest of the front seat.

88.3	212.5	290.2	347.3	393.4	434.9	480.9	517.6	549.0	596.7
126.5	234.2	298.8	350.3	399.6	439.5	490.5	522.9	555.5	598.6
144.7	245.0	304.8	362.8	407.8	446.0	500.7	526.8	568.4	
154.6	255.9	308.9	369.6	410.9	453.6	506.4	530.6	577.8	
172.2	269.2	318.4	375.5	422.5	463.0	508.4	534.2	583.3	
192.6	277.7	323.2	381.1	426.6	464.3	514.1	538.3	589.5	
197.3	285.8	329.5	390.3	430.2	470.7	515.1	544.8	594.1	

Table 4.3: Eigenfrequencies of the acoustic domain of fig.(4.2) in the range [0-600] Hz

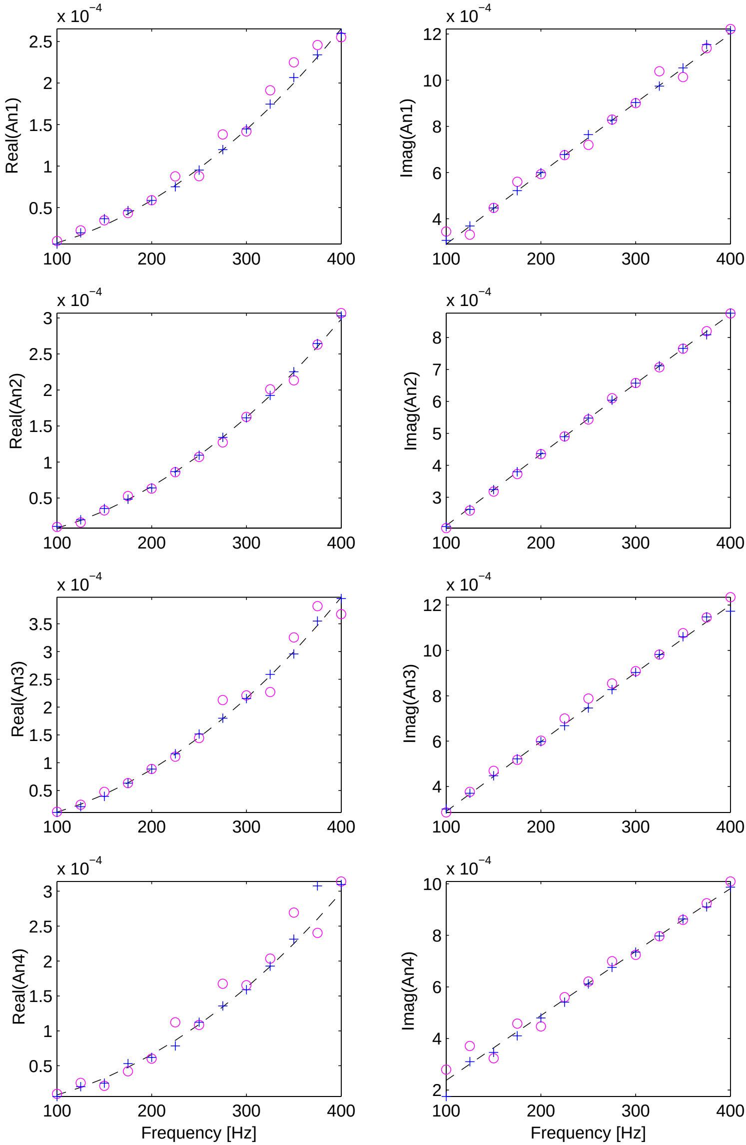

Figure 4.3: Updated admittance coefficients with 5% measurement noise ('o' plot symbols) and without noise ('+' plot symbols); the dotted line draws the reference values

The surface bounding the acoustic domain which is not covered by absorbing materials is assumed to be rigid, with the exception of the firewall that vibrates with a normal velocity $v_0 = 1mm/s$ and constitutes the only acoustic source. Fig. (4.2) highlights the geometry together with the vibrating firewall and the damping boundary conditions.
The device is updated in the frequency range [100-400] Hz and the modal basis makes use of eigenvectors up to 600 Hz. The corresponding natural frequencies of the setup are reported in table (4.3). The admittance coefficients are updated every 25 Hz, and the initial values of the admittance coefficients at the first iteration of the optimization process are set to the double of their exact values. iThe nodal pressure is recorded at 50 different locations randomly distributed into the acoustic domain to simulate the measurements.
The updating process is applied twice to the setup. During the second run, the reference finite element pressure field replacing the measurements is polluted numerically in order to simulate a slight discrepancies in the experimental data. The noisy reference field is obtained by multiplying the real and imaginary parts of each measurement by $1 + \omega * N$, where N is a random number chosen from a normal distribution with mean zero and variance one, and ω is the weight applied to the normal distribution, and so the average noise level that is set to 5%.
The updated admittance parameters are plotted in fig.(4.3). Both the real and imaginary parts of the coefficients are reported and compared to the exact values while updating the model with and without measurement noise. The corresponding errors on the admittance magnitude are shown in fig.(4.4): the maximum error level is about 5% with perfect experimental data, and it never reaches 10% when polluting the reference pressure field. The average values over the frequency range are significantly lower.
Fig.(4.5) draws the residual constitutive law error after updating along the frequency range of interest. The CLE varies between 1 and 8.5% with noisy measurements, and it drops significantly when using perfect experimental data. The CPU time speedup is also plotted in fig.(4.5). It is computed by the ratio of the running time of the full non reduced model updating process at a given frequency and the corresponding time while projecting the model into the subspace, and this ratio moves around 110. Actually, the number of iterations needed for updating the setup at a given frequency is about the same while using the full or the reduced model (around 300 iterations).

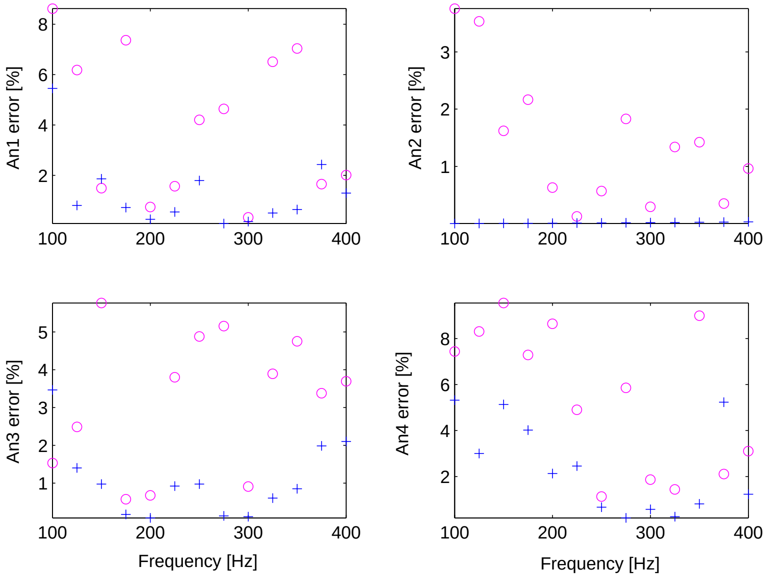

Figure 4.4: Updated admittance coefficient error with 5% measurement noise ('o' plot symbols) and without noise ('+' plot symbols)

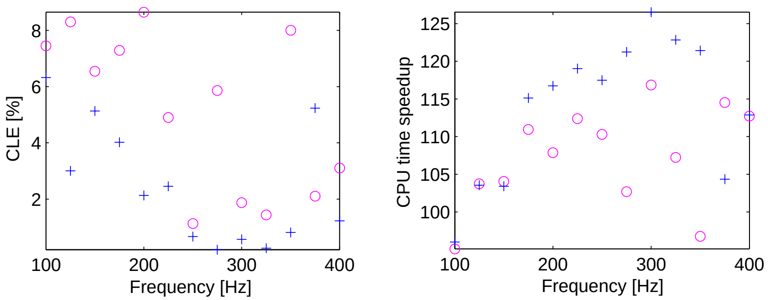

Figure 4.5: CLE residue after updating and CPU time speedup (full/reduced model updating time ratio): updating with 5% measurement noise ('o' plot symbols) and without noise ('+' plot symbols)

So, the speedup to update the system at each frequency is close to the ratio of the CPU times needed to compute one single iteration with the full and the light models. Note that the full model computations are achieved in a optimized way, taking advantage of the sparse property of the finite element matrices and using a skyline solver to invert the system of equations. The initial sparse system size is 39450 (twice the number of nodes) while the reduced non-sparse equation set size is 818 (twice the number of vectors in the reduced basis).
The order of magnitude for the time needed to update the 20.000 node models on a single 2.4 GHz Linux processor is around 4 minutes for each frequency when using the reduced basis. It yields to somewhat less than one hour to update the system in the [100-400] Hz frequency range with an increment of 25 Hz. With a deceleration of ca. 110, the entire non reduced model updating process runs for four days.

4.5 Conclusions

The paper discusses the problem of validating large acoustic setups of industrial size by the mean of the constitutive law error technique. In order to update such models, the optimization problem is rewritten under the form of a system of undamped forced vibration problems.
That leads us to build a reduced basis with the following contributions:

- a truncated modal basis,
- the static response of the system to the excitation of the acoustic domain (Krylov series),
- static responses to the forces related to the variations of the system during the updating process,
- static responses associated to the measured degrees of freedom

The reduced basis is implemented and tested on two numerical examples. The paper presents a very simplified model of a 3D car cabin: the updating of the model is achieved using 3 different bases, the first being a classical truncated modal basis, and the others adding progressively the static contributions listed above. Comparing the results of the 3 validations shows that a very good quality for the updating process is only reached when the reduced basis is used with all the contributions proposed in the paper.

A second application deals with a pretty similar geometry but with a refinement of about 20.000 nodes. The absorbing materials covering the roof, the floor and the the back-rest of both the front and the rear seats of the car are updated with and without measurement noise. A detailed analysis of the numerical results is presented. Compared to the validation step that uses the full non reduced model, the CPU-time of the reduced updating process is about 110 times lower for this setup of average size.

Chapter 5

Updating 3D acoustic models with the CRE method: a two-stage approach for absorbing material characterization [1]

Contents

[1] This chapter is reproduced from: V. Decouvreur, P. Ladevèze, and Ph. Bouillard. Updating 3D acoustic models with the constitutive relation error method: a two-stage approach for absorbing material characterization. Journal of Sound and Vibration (accepted for publication), 2007.

In the global framework of improving vibro-acoustic numerical simulations together with the need to decrease the number of prototyping stages, improving the quality for acoustic models becomes increasingly important for many industries such as automotive companies, for instance. This paper focuses on achieving greater accuracy for acoustic numerical simulations by making use of a parametric updating technique, which enables tuning the model parameters inside physically meaningful boundaries. The improved model is used for the next prototyping stages, allowing more accurate results within reduced simulation times. The updating technique used in this paper is based on recent works dealing with the constitutive relation error method (CRE) applied to acoustics. The updating process focuses on improving the acoustic damping matrix related to the absorbing properties of the materials covering the borders of the acoustic domain.
The present study proposes a 2-stage optimization process, which exhibits many advantages. Indeed, the computational time decreases, the frequency interpolation of the material absorbing properties outside the studied frequency range is easily performed, and comparing the correlation of several material absorbing constitutive equations with experimental records is fast.
Additional originality of the work comes with the application of the CRE updating method to a concrete real-life device, while previous works addressed purely numerical setups without experimental data. The test-case is the TRICARMO setup engineered by LMS International in Leuven, Belgium. The TRICARMO setup is a simplified car cabin with rigid walls and car seats inside. Thanks to the 2-stage approach, the material property characterization of the seat is improved by running the updating simulation process using a physical absorbing material model.

5.1 Introduction

In recent years, many industries have taken into account noise control consideration during the design stages, either to satisfy code rules or to improve the end-user's comfort. To evaluate and further improve the numerical model, experimental information remains highly useful.
Updating techniques aim at getting numerically simulated physical fields that are closer to the measured ones. Among these techniques, some act on tuning model parameters inside physically meaningful boundaries. Such methods allow to use the new parameters in further computations while changing the

configuration.
In [DBDL04a], the choice of using the constitutive relation error (CRE) method to update acoustic models is motivated, and the principles of the CRE are extensively explained. The technique is also applied to 2D academic test-cases. The good results encouraged the authors to apply the CRE technique to 3D real-life test cases, but the developed technique showed a drawback in terms of computational time. Indeed, the CRE updating technique requires solving a matrix system that is larger than the initial one. Furthermore, the technique being iterative, several hundred inversions of the larger matrix are performed for each frequency. One of the goals achieved by the 2-stage approach presented here is to decrease the running time.
To face real-life test cases, the admittance model that is used to evaluate the absorbing properties of the porous materials has to be as accurate as possible. The present paper uses Wilson's admittance formulation ([Wil97]) to characterize the porous compounds of the numerical applications.
The clue of the updating technique presented here is to split the updating process into a first stage that has to be independent of any admittance model, and a second stage that links the microstructural material properties to the material absorbing behavior through an admittance model, as explained in chapter 5.2. In the first stage, each absorbing material is characterized by a single complex number for each updating frequency.
In the second stage, a physical admittance model is used to fit as well as possible the real and imaginary parts of the admittance coefficients that have been found thanks to the first stage. This fitting stage is processed through the studied frequency range for each absorbing material.
With the goal to compare several admittance models when updating an acoustic setup, the frequency correlation with the updated admittance coefficients using a specific absorption model during the second stage is treated like a post treatment analysis and is very cheap in terms of CPU time.
Mathematical foundation of the CRE updating method is formulated in chapter 5.1.1. The wall admittance modeling is described in paragraph 5.1.2, and part 5.1.2 presents the admittance model of Wilson that will be used later to update the numerical applications treated in the article.
The 2-stage approach detailed description together with a validation study are parts of chapter 5.2.
Chapter 5.3 addresses the updating of a real-life device : a concrete simplified car engineered by LMS International, which is called TRICARMO. Car seats are placed into the setup and are the only absorbing facilities damping the

acoustic waves inside the TRICARMO car. The setup is instrumented with many microphones recording the sound pressure level inside the car.
The 2-stage updating technique is used to update the driver's seat absorbing properties through a frequency range that goes from 50 to 350 Hz.
Finally, chapter 5.4 presents the conclusions about the ability of the 2-stage updating approach to accurately improve the numerical simulation of acoustic absorbing properties.

5.1.1 Updating acoustic models with the CRE

The present paper uses a parametric updating technique based on the constitutive relation error (CRE). The fundamentals of the CRE were first developed by P. Ladevèze in structural dynamics (see [Lad98]) and then applied to acoustics in [DBDL04a]. The main idea in the CRE technique consists in splitting the data and equations of the model into 'reliable' information and 'less reliable' one. Whether one trusts a given data or equation has to be related to the assumptions made in its derivation.

The reliable information

A solution has to verify the reliable information exactly. In what concerns acoustics, it means that the pressure field p has to satisfy the Helmholtz wave equation with the associated Dirichlet and Neumann boundary conditions on parts $\partial_1\Omega$ and $\partial_2\Omega$ of the boundary respectively:

$$\begin{cases} \text{Helmholtz : } \Delta p + k^2 p = 0, \\ \text{Dirichlet B.C.: } p_{|\partial_1\Omega} = \overline{p}, \\ \text{Neumann B.C.: } v_{n_{|\partial_2\Omega}} = \dfrac{\mathrm{j}}{\omega\rho}\dfrac{\partial p}{\partial n}|_{\partial_2\Omega} = \overline{v}_n, \end{cases} \tag{5.1}$$

where $\mathrm{j} = \sqrt{-1}$, ω is the angular frequency, k is the wave number, ρ is the fluid density, v_n is the normal velocity, and $\overline{p}$ and $\overline{v}_n$ are the imposed pressure and normal velocity on parts $\partial_1\Omega$ and $\partial_2\Omega$ of the boundary respectively.

The less reliable information

The best candidate among a solution set satisfying the reliable information minimizes the constitutive relation error estimator, which is built on the less reliable information.

In particular, through this paper, it is chosen that the Robin admittance boundary condition together with the measured pressure field amplitude will not be verified exactly, assuming that those data are the most questionable for the present acoustic model. Practically, the pressure field q will satisfy the Robin equation (5.2), and the distance between pressure variables p and q will be minimized.

$$\text{Mixed Robin B.C.: } v_{n_{|\partial_3\Omega}} = A_n(\omega)q, \tag{5.2}$$

where A_n is the admittance coefficient, and $\partial_3\Omega$ defines the absorbing boundary where equation (5.2) applies. As to the uncertainty on the measured pressure levels, discrepancies between computed pressure p and measured field $\tilde{p}$ has to be minimized also.
The two contributions to the less reliable information result in building the error estimator CRE (5.3).

$$e_\omega^2 = \omega^2\rho^2 \int_{\partial_3\Omega} (v_n - A_n q)^*(v_n - A_n q)d\Gamma + \frac{r}{1-r}\|p - \tilde{p}\|^2, \tag{5.3}$$

where $v_n = \dfrac{\mathrm{j}}{\omega\rho}\dfrac{\partial p}{\partial n}$ and $(.)^*$ denotes the complex conjugate. The weighting factor $\dfrac{r}{1-r}$ is related to the confidence in the measurements in comparison with the model accuracy. In the absence of a priori knowledge in the measurement quality, r is set to 0.5, keeping in mind that $0 \leq r < 1$.

Discrete formulation of the CRE updating method

The continuous acoustic model can be approximated by a discrete formulation, e.g. using the finite element formalism based on a variational form of reliable equations (5.1) and (5.2). Updating the approximated discrete model is achieved by solving the finite element matrix equation while minimizing the CRE estimator, as presented in (5.4).

$$\text{Find } s_\omega{=}(\mathbf{P},\mathbf{Q}) \mid \quad \left\{ \begin{array}{l} [\mathbf{K}]\mathbf{P} + \mathrm{j}\omega\rho[\mathbf{C}]\mathbf{Q} - \omega^2[\mathbf{M}]\mathbf{P} = [\mathbf{E}]\mathbf{P}, \\ e_\omega^2(s_\omega) \text{ is minimum,} \end{array} \right. \tag{5.4}$$

where the discrete form of the modified CRE (5.3) taking into account the experimental error is given by:

$$e_\omega^2 = \omega^2\rho^2(\mathbf{Q}-\mathbf{P})^*[\mathbf{D}](\mathbf{Q}-\mathbf{P}) + \frac{r}{1-r}(\mathbf{\Pi P} - \tilde{\mathbf{P}})^*[\mathbf{G_w}](\mathbf{\Pi P} - \tilde{\mathbf{P}}). \tag{5.5}$$

The definition of the finite-element vectors and matrices is as follows:

- $p^h = \mathbf{N}^t\mathbf{P}$ and $q^h = \mathbf{N}^t\mathbf{Q}$ are approximated pressure fields ($\mathbf{N}$ being the shape functions),
- $[\mathbf{M}] = \frac{1}{c^2}\int_\Omega \mathbf{N}^t\mathbf{N}d\Omega$ is the mass matrix (c being the sound speed),
- $[\mathbf{K}] = \int_\Omega \nabla^t\mathbf{N}\nabla\mathbf{N}d\Omega$ is the stiffness matrix,
- $[\mathbf{C}] = \int_{\partial_3\Omega} A_n\mathbf{N}^t\mathbf{N}d\Gamma$ is the admittance matrix,
- $[\mathbf{E}] = \int_{\partial_2\Omega} \nabla_n{}^t\mathbf{N}\mathbf{N}d\Gamma$ is the system excitation matrix due to normal velocities prescribed on boundary $\partial_2\Omega$,
- $[\mathbf{D}] = \int_{\partial_3\Omega} A_n^*A_n\mathbf{N}^t\mathbf{N}d\Gamma$.

$[\mathbf{G_w}]$ represents the error measure $\|.\|^2$ of equation (5.3), $\mathbf{\Pi}$ is a projection operator that gives the value of the pressure at the corresponding sensors, and $\tilde{\mathbf{P}}$ is the nodal value vector of the measured pressure $\tilde{p}$.
In the numerical example of this paper, $[\mathbf{G_w}]$ is a square unity matrix of size equal to the number of measurements.
The updating process is iterative: each step consists in computing new updating parameters and solving the problem using these new values. The computed pressure is compared to the measurements using the constitutive relation error, and the iterative process stops when the error is below a reference threshold value.

5.1.2 Modeling of the wall admittance

The sound absorption in porous media consists of 3 different contributions ([All93]):

- the viscous effects in the boundary layer close to the frame,
- the thermal diffusion process between the fluid and the frame,

- the internal energy losses coming from the frame motion.

The main geometrical parameters of these absorbent materials are:

- the porosity $\Omega = V_f/V_t$, where V_f and V_t are the fluid volume and the total volume respectively,
- the tortuosity q,
- the average pore diameter d [m],
- the flow resistivity σ [Nm^{-4}s].

Absorbing media and equivalent fluid

The modeling of the absorbing media is based on the concept of equivalent fluid (see [All93]). The heterogeneous porous medium is made of a skeleton/frame perforated by pores with various shape. Though, it is regarded as an homogeneous fluid, which is characterized by a complex propagation constant Γ, a complex impedance Z_c and a thickness d_e (see fig. 5.1). The local phenomena occurring inside the absorbing material are not modeled. An acoustic wave entering the material is supposed to be reflected and to exit the material at the incidence location. This assumption is perfect for waves entering the medium perpendicularly to its surface. The outgoing acoustic wave is computed from the incident wave and the wall impedance representing the absorbing medium. If the incident wave enters the absorbing medium perpendicularly to its surface, the wall admittance Z_n is given by equation (5.6).

$$Z_n = Z_c \frac{Z_c - \dfrac{\mathrm{j}Z_{n0}}{tan(\Gamma d_e)}}{Z_{n0} - \dfrac{\mathrm{j}Z_c}{tan(\Gamma d_e)}}, \tag{5.6}$$

where Z_{n0} is the wall admittance of the surface backing the absorbing material. In the particular case where the layer of equivalent fluid is backed by a rigid impervious wall, $Z_{n0} \to \infty$, and equation (5.6) reduces to (5.7).

$$Z_n = \frac{-\mathrm{j}Z_c}{tan(\Gamma d_e)}. \tag{5.7}$$

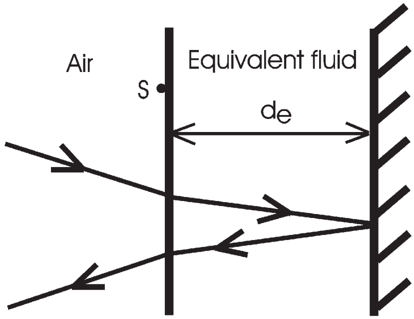

Figure 5.1: Layer of equivalent fluid (thickness d_e) representing an absorbing material backed by a rigid impervious wall

Admittance models in the literature

The admittance models presented in the literature can be split in 3 kinds of models:

- the empirical models,
- the microstructural models,
- the phenomenological models.

The microstructural models are derived by calculating the exact solution for the propagation of sound waves in pores of constant circular cross section. The resulting equations are tuned to accommodate more complicated geometries using one or two shape factors. While microstructural models provide a quite accurate absorption description for a broad range of frequencies and materials, their equations are very complicated to handle and require many experimental data to be provided.
Phenomenological models propose a compromise between microstructural and empirical models: they are derived from simplified propagation models inside porous media. They provide relations for Γ and Z_c that usually describe the absorbent materials nearly as well as microstructural models do. Hence, phenomenological models are easier to handle and less experimental information is required. Additional information about admittance models can be found in the literature of [Wil97].

Wilson's model

Wilson's model is particularly interesting in the framework of updating updating materials because it can be described by 1, 4 or 5 parameters, and the model is able to mimic the frequency behavior of any empirical or microstructural admittance model. Wilson's equations describe the propagation of sound in porous materials as follows ([Wil97]):

$$\frac{Z_c}{\rho c} = \frac{q}{\Omega}\left[\left(1+\frac{\gamma-1}{\sqrt{1-\mathrm{j}\omega\tau_{ent}}}\right)\left(1-\frac{1}{\sqrt{1-\mathrm{j}\omega\tau_{vor}}}\right)\right]^{-1/2}, \tag{5.8}$$

$$\frac{\Gamma}{\omega/c} = q\left[\left(1+\frac{\gamma-1}{\sqrt{1-\mathrm{j}\omega\tau_{ent}}}\right)/\left(1-\frac{1}{\sqrt{1-\mathrm{j}\omega\tau_{vor}}}\right)\right]^{1/2}, \tag{5.9}$$

where ρ is the fluid density, c is the sound velocity, γ is the specific heat ratio, q is the tortuosity, Ω is the porosity, and σ is the flow resistivity, an intrinsic property of the material that measures the resistance to an air flow through it. σ lies between 5000 and 10^5 $\mathrm{Nm}^{-4}\mathrm{s}$ for materials like fiberglass and open-bubble foam.
τ_{ent} is the relaxation time (i.e. the time necessary to return to an equilibrium state after a perturbation is introduced) related to the temperature gradient between the fluid and the frame. τ_{vor} is the relaxation time of the pressure gradient related to the fact that the fluid sticks to the frame.
By default, Wilson's model exhibits 4 parameters which are q, Ω, τ_{ent}, and τ_{vor}. With $X = \dfrac{\rho f}{\sigma}$ being the reduced frequency and $f = \dfrac{\omega}{2\pi}$ the frequency, the model of Wilson supposes to evaluate τ_{ent} and τ_{vor} at low and high reduced frequencies, let say at $X = 0.01$ and $X = 1$. Interpolating between these reduced frequency values gives the characteristic impedance and the propagation constant at mid frequencies. If one is interested in a given microstructural model, it is possible to mimic its behavior by computing τ_{ent} and τ_{vor} by making use of the equations for Z_c (5.8) and Γ (5.9).
In the particular case of the well known Delany-Bazley model ([DB70]), it is assumed that $\Omega = 1$ and $q = 1$. This is actually in good agreement with that simple model. Since this empirical model exhibits only one material dependent parameter, τ_{ent} and τ_{vor} are computed at the average reduced frequency $X = 0.1$. The system of 2 equations (5.8, 5.9) with 2 unknowns then yields to relations (5.10) and (5.11), which are functions of the reduced frequency, and

then of the flow resistivity only.

$$\frac{Z_c}{\rho c} = \left[\left(1+\frac{\gamma-1}{\sqrt{1-\mathrm{j}19X}}\right)\left(1-\frac{1}{\sqrt{1-\mathrm{j}13X}}\right)\right]^{-1/2}, \tag{5.10}$$

$$\frac{\Gamma}{\omega/c} = \left[\left(1+\frac{\gamma-1}{\sqrt{1-\mathrm{j}19X}}\right)/\left(1-\frac{1}{\sqrt{1-\mathrm{j}13X}}\right)\right]^{1/2}. \tag{5.11}$$

In chapter 5.3.3, one uses Wilson's model for which τ_{ent} and τ_{vor} are computed by comparing relations (5.8) and (5.9) to the microstructural model of Biot-Allard [ADN+90] at low and high frequencies. The relaxational times solving the equalities are:

$$\tau_{vor} = 2\frac{\rho q^2}{\Omega\sigma}, \tag{5.12}$$

$$\tau_{ent} = N_{Pr} S_b^2 \tau_{vor}, \tag{5.13}$$

where N_{Pr} is the Prandtl number. That version of Wilson's model needs 4 absorbent material dependent parameters like the initial one of Biot-Allard. These parameters are the porosity Ω, the tortuosity q, the flow resistivity σ, and a shape factor S_b.

5.2 The 2-stage approach

5.2.1 Principles

The 2-stage updating method splits the process in 2 phases. Compared to the CRE technique presented in chapter 5.1.1, the 2-stage approach solves the same system of equations (5.4). The main difference resides in the optimization loop aiming at minimizing the error estimator (5.5).
In the former CRE updating technique, the optimization process uses a classical gradient based method to chose the next candidate for each admittance coefficient. The choice consists in evaluating the gradient of the error estimator (5.5) with respect to each parameter of the admittance coefficients to find the best optimization direction minimizing the CRE. The time needed to find the next best candidate from iteration k to $k+1$ is proportional to the number of parameters characterizing each absorbing material.
The first stage of the new updating technique then reduces the running time by characterizing each admittance coefficient using only two variables : the real

and imaginary parts. Indeed, most of the admittance models use at least four intrinsic parameters to determine the absorbing properties of a given porous material. Knowing also that increasing the number of optimization parameters makes the search of the optimum solution more difficult, reducing the size of the variable space yields to stabilizing the optimization process. The first stage is run at a few frequencies evenly spread within the studied frequency range. Then, the second step is launched to get a continuous description of each admittance coefficient through the frequency range. Based on an admittance model that is parameterized in terms of frequency and intrinsic structural material properties, the second stage consists in finding the best combination of parameters that generates a smooth frequency interpolation of the discrete set of real and imaginary parts found during the first stage. The fitting process of the second stage is once again based on a gradient optimization technique. This stage is though much faster since the functional to be minimized is the distance between two admittance coefficients while during stage one, each evaluation of the error estimator requires solving the finite element system of equations. For each absorbing material, the second stage can be written following expression (5.14).

$$\text{Find } s = (\alpha_m)_{|(m=1,\ldots,M)}| \quad \sum_{l=1}^{L} \|A_{n,l}^{up} - A_{n,l}(\omega, s)\| \quad \text{is minimum,} \tag{5.14}$$

where:

- α_m are the intrinsic parameters of the admittance model with $m = 1, \ldots, M$,
- L is the number of updating frequencies,
- $A_{n,l}^{up}$ is the updated complex admittance coefficient from stage 1,
- $A_{n,l}(\omega, s)$ is the admittance coefficient computed using a frequency dependent model based on structural parameters α_m.

In summary, the first stage looks for the best complex admittance coefficient for each material of the setup at a given frequency. The introduction of a particular admittance model is achieved through the second stage, which fits the complex admittance coefficients that were calculated during the first updating stage through the frequency range of interest. The variable parameters of the admittance model are physical properties of the absorbing material and can vary inside plausible boundaries.

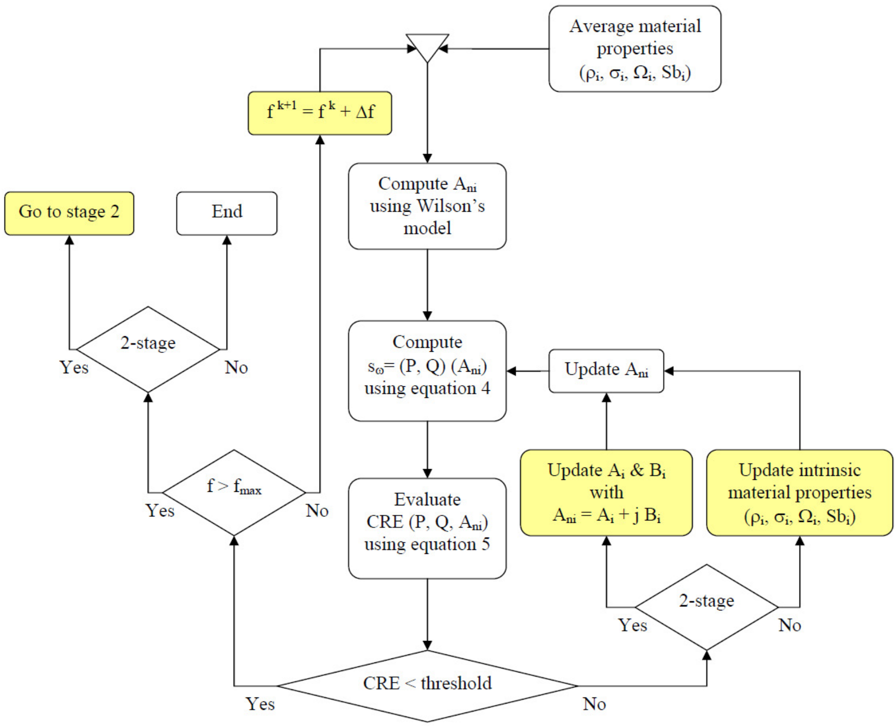

Figure 5.2: Flowchart of the conventional CRE updating method versus the 2-stage approach

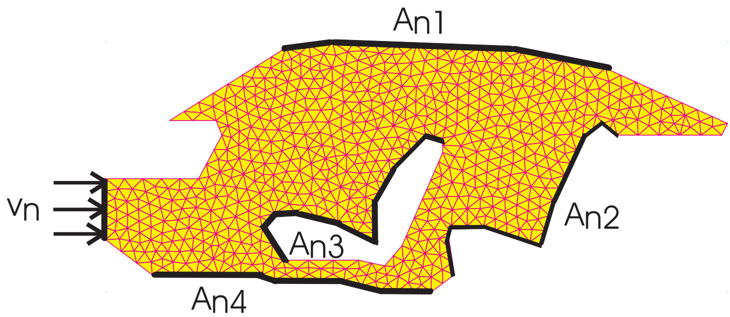

Figure 5.3: Academic setup used to validate the 2-stage method : the car cabin is equipped with 4 absorbing materials $A_{n1\rightarrow 4}$ and the noise inside the acoustic domain is generated by the dashboard vibrations with normal velocity v_n

5.2.2 The 2-stage approach vs. the former CRE method

A flowchart comparing the former CRE updating technique versus the 2-stage version is presented in fig. 5.2. The darker boxes highlight the differences between the two CRE based updating technique process flows.
From top to bottom in fig. 5.2, the first discrepancies concern the frequency increment Δf between two updating frequencies. The 2-stage technique allows for larger frequency increments since a frequency dependent admittance model is used during the fitting step of the second stage.
The second darker box indicates the use of a second stage only for the new updating process flow.
The bottom dark boxes explain the differences in the gradient based optimization process of the first stage as mentioned in paragraph 5.2.1 : the former updating technique calculates partial derivatives of the functional with respect to structural parameters of the absorbing materials, while the 2-stage approach considers only the derivatives with respect to the real and imaginary parts of the admittance coefficients.

5.2.3 Validation of the 2-stage technique

The goal of this part is to validate the 2-stage technique on a simple academic model inspired from [Nef82]. The setup is a two dimensional car cabin that

is covered with 4 different absorbing materials and excited by its firewall as described in fig. 5.3. The absorption of the 4 layers is characterized using a 4 parameter Wilson's model with standard material properties for porous foam. The thickness of layers 1 to 4 is 3, 4, 5 and 6 cm respectively, and the corresponding material properties are initially determined to build a finite element reference pressure field that replaces the experimental data.
Then, the setup is updated to find back the right admittance properties, the initial values being voluntarily biased by about 30 percents. The updating frequency range goes from 50 to 500 Hz.
The device is firstly updated using a standard CRE method, which means using a 4 parameter description of the absorbing materials (Wilson's model) and a frequency increment of 10 Hz for instance.
Then, the 2-stage technique is applied to the academic device, updating the absorbing materials using its real and imaginary parts and a frequency increment of 40 Hz. The fine frequency description of the admittance coefficients is obtained thanks to the second stage of the method that smoothes the discrete admittance values using its 4 parameter description.

Admittance coefficient	Porosity Ω	Tortuosity q	Flow resistivity σ [Nm^{-4}s]	Shape factor S_b
$A_{n1\rightarrow4}$	0.95	1	10000	1

Table 5.1: Microstructural parameters of the absorbing materials for the academic setup 5.3

On this simple example, the 2-stage technique runs 15 times quicker than the standard one. The quality of the results is examined in fig. 5.4 by looking at the frequency plot of the 4 admittance coefficients provided by both updating techniques. The discrete values computed using the standard updating technique (tick marks in fig. 5.4) and the smoothed interpolation calculated via the 2-stage approach (based on raw data that are not represented in fig. 5.4) match perfectly, which validates the fast 2-stage method.
The microstructural parameters characterizing the absorbing materials that are used to build the reference pressure field are reported in table 5.1. The same microstructural properties are used for all materials, the only changing parameter being the layer thickness, which is sufficient to change the admittance properties of the absorbing materials. The discrepancy between the reference

parameters and the updated ones never reaches 1% no matter the updating technique, so that only reference values are presented in table 5.1.

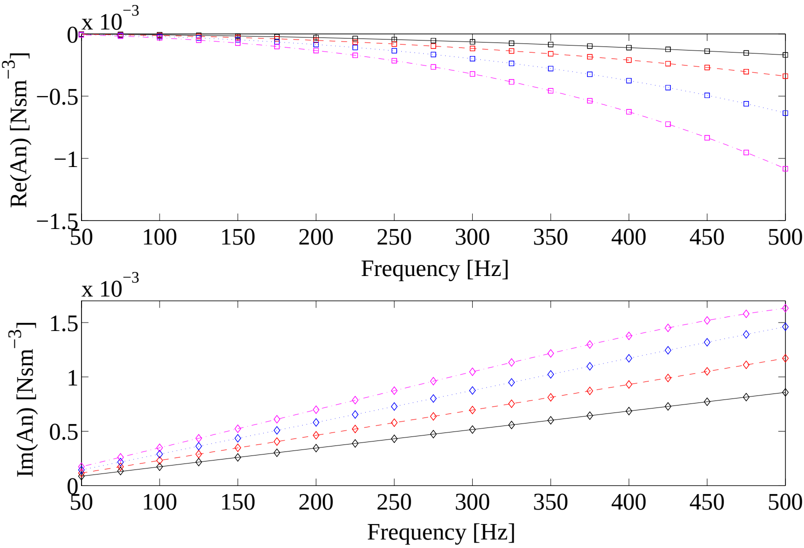

Figure 5.4: Admittance coefficients computed with the standard discrete updating method (tick marks), and with the 2-stage approach (lines). Material 1, solid line; material 2, dashed line; material 3, dotted line; material 4, dash-dotted line

5.3 Updating a real-life test case setup

5.3.1 TRICARMO setup description

The TRICARMO setup is a simplified concrete car cabin that has been developed by LMS International in Leuven (see fig. 5.5) in the framework of a research project founded by the Flemish Institute for the promotion of scientific and technological research in industry (IWT) [BBKD02]. The acoustic domain is excited by a loudspeaker that simulates the vibration of the dashboard, and a driver's seat lies in the car cabin. Experimental pressure fields to be used in the first updating stage are recorded in a few locations of the acoustic domain. The updating process aims at characterizing the absorbing properties of the seat.

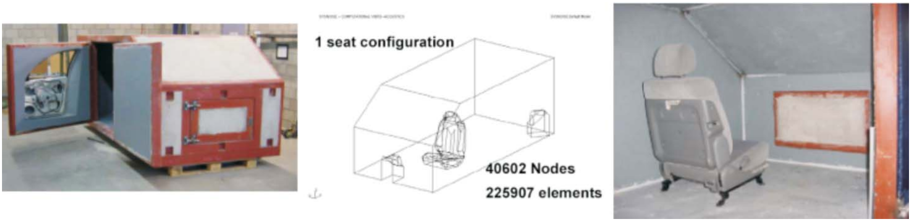

Figure 5.5: TRICARMO concrete car with driver's seat (courtesy of LMS International)

5.3.2 Driver's seat modeling

The TRICARMO setup can be equipped with different seat configurations. While it is possible to achieve measurements with front and rear seats inside the concrete car, the results presented here focus on the "driver's seat only" configuration.
The seat modeling is split into a backrest and an horizontal cushion. Both cushions are represented by a two layer material. The bottom layer is a thick open cell foam (material 1 in fig. 5.6). The top layer consists of a thin foam layer covered by a fabric skin (materials 2+3 in fig. 5.6). The cover fabric is not modeled separately and materials 2+3 in fig. 5.6 are merged together in one absorbing material for the numerical simulations. So, each seat cushion is regarded as the superposition of two absorbing materials with admittance coefficients A_{n1} and $A_{n(2+3)}$ and the equivalent wall admittance of the assembly is computed using equation (5.6).
The backrest and bottom cushion average thickness is respectively 60 and 55 mm. In both cases, material 2+3 accounts for 8.25 mm of the total thickness of the cushion. Samples of those materials were analyzed by the "Laboratorium voor Akoestiek en Thermische Fysika" of the Catholic University of Leuven (K.U.L.), Belgium. Material properties such as density, tortuosity, porosity,

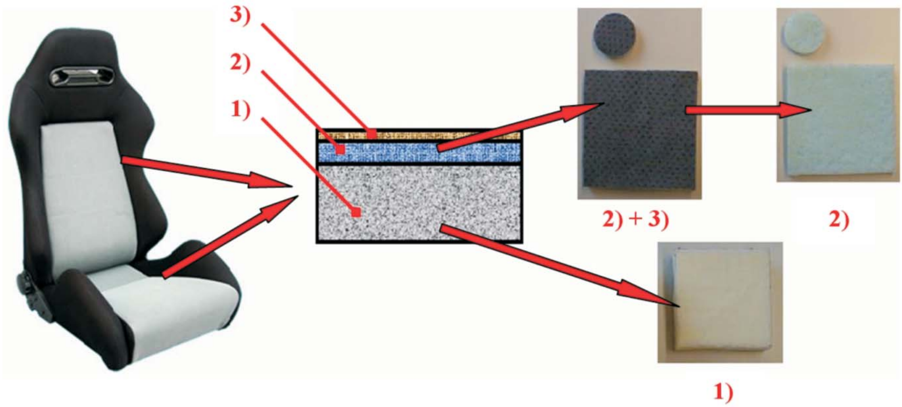

Figure 5.6: Car seat analysis : backrest and bottom cushions are modeled by layers of porous materials. 1) thick open cell foam, 2) thin foam layer, 3) fabric skin (material sample pictures from [KJL01])

flow resistivity, etc., were evaluated to run deterministic numerical simulations with highly refined seat mesh in the framework of other studies. Some of these material properties will be used to check the updated results of the present analysis.

5.3.3 Updating results

The updating process looks for the best parameter combination to describe the frequency behavior of the absorbing materials of the seat. The updating is achieved through a frequency bandwidth of [50-350] Hz with a frequency step of 25 Hz. Running the first stage provides the complex discrete admittance coefficients at frequencies 50, 75, 100, ... , 350 Hz. Running the second stage then needs to choose an admittance model. For instance, this stage is run first with an empirical Delany-Bazley model, and then with a 4 parameter Wilson's phenomenological admittance model based on the Biot-Allard's microstructural one. Initial values for the parameters at the first iteration are set to $\Omega = 1$, $q^2 = 1$, $\sigma = 10^4$ Nm^{-4}s, and $S_b = 1$. As discussed before, the second stage is very cheap in terms of CPU time compared to the first stage, as shown in

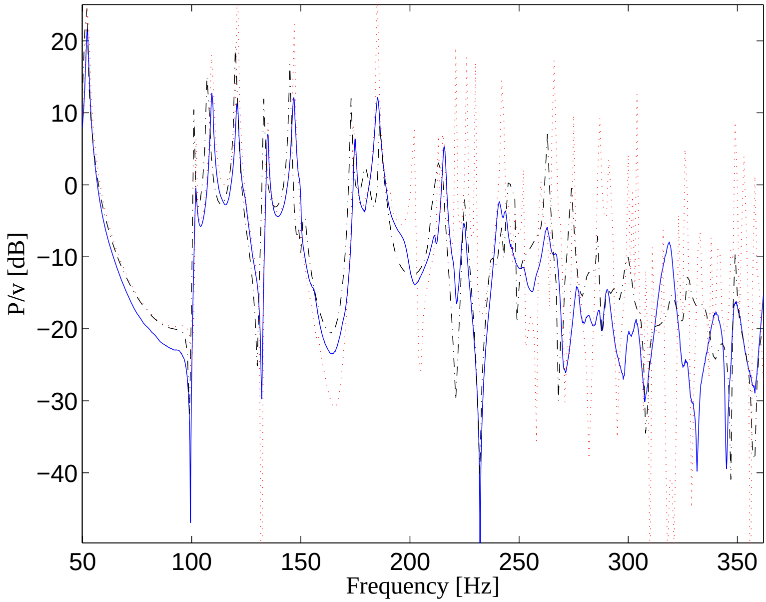

Figure 5.7: Pressure/velocity ratio at the driver's ear : measured (solid line), computed without absorption from the seat (dotted line), and computed with updated absorption properties of the seat (dash-dotted line)

table 5.2 where the second stage typically accounts for about 1% of the total computational time. The entire updating process runs for 2 hours on a single 2.4 GHz Linux processor.

The second stage provides continuous values of the admittance coefficient from the discrete updated results. The smooth values are used to build the updated pressure field at the driver's ear in fig. 5.7. The updated pressure/velocity ratio, which is called mobility, is plotted (actually its amplitude, in dB) together with the experimental curve and the ratio computed without taking into account the absorbing properties of the seat (i.e. the undamped dotted FRF, fig. 5.7). The updated FRF (dash-dotted line) fits rather well the measured one (solid line). This result could not necessarily have been foreseen since no information was provided for the porous material of the seat excepted its average

	stage 1	stage 2 (Delany-Bazley)	stage 2 (Wilson)
CPU time [%]	98.1	0.8	1.1

Table 5.2: Relative CPU time comparison for the different stages: stage time/total updating time

thickness. Though, for this particular case, the slow frequency dependence of the homogenized parameters characterizing the porous media potentially improves the result quality of the method (see fig. 5.8).
The updated material properties of the seat yield to admittance coefficients that are compared to the coefficients coming from the material properties measured in the lab. The comparison in fig. 5.8 deals with the real and imaginary parts of the admittance coefficients of the backrest and bottom cushions of the seat. The real and imaginary parts computed with the measured material properties are slightly different from the ones calculated with the updated material characteristics. That can be partially explained by the fact that most of the measurement techniques do not take into account the tridimensional behavior of the tested material sample.

	Porosity Ω	Tortuosity q	Flow resistivity σ [Nm^{-4}s]	Shape factor S_b
A_{n1} (measured)	> 0.95	1.28	9053	-
$A_{n(2+3)}$ (measured)	> 0.95	1.16	7282	-
A_{n1} (updated)	0.99	1.32	10505	1.05
$A_{n(2+3)}$ (updated)	0.99	1.19	7337	0.86

Table 5.3: Measured versus updated microstructural parameters of the porous media

The resulting microstructural parameters of the porous media are reported in table 5.3 together with the experimentally measured material properties. The shape factors cannot be measured, which explains why there is no corresponding data in table 5.3.
For this particular setup, the backrest and bottom cushions are made of the same absorbing material, the only difference being the thickness of the cushions. Then, during the second stage optimization process, the backrest and

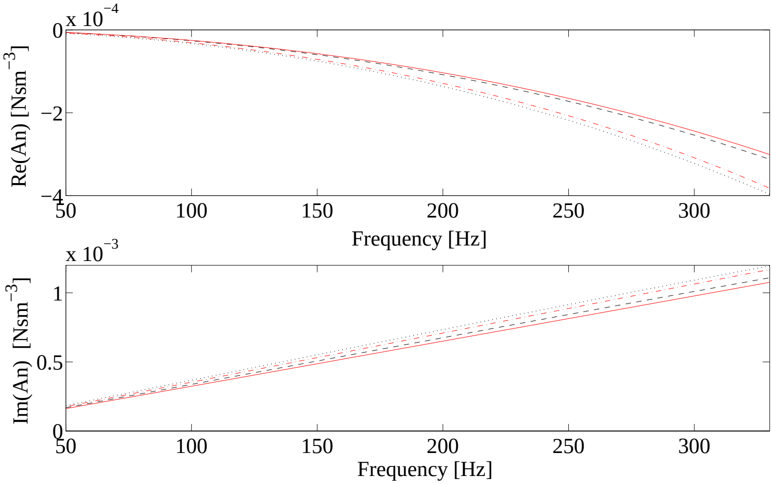

Figure 5.8: Real and imaginary parts of the admittance coefficients of the backrest and bottom cushions constituting the seat computed with the measured and the updated microscopic properties. Measured bottom cushion, dashed line; updated bottom cushion, solid line; measured backrest cushion, dotted line; updated backrest cushion, dash-dotted line

bottom cushions are updated simultaneously, and the intrinsic properties of the materials are imposed to be identical for both cushions.
It is also interesting to compare the FRF built using the updated admittance values to the FRF based on the initial guest that would be used if no experimental data were available and the updating process was not performed (i.e. $\Omega = 1$, $q^2 = 1$, $\sigma = 10^4$ Nm^{-4}s, and $S_b = 1$). Figure 5.9 presents the mobility at the driver's ear. The experimental mobility is compared to the mobility computed using standard material properties and using the updated values. In bottom graph of fig. 5.9, the authors want to quantify the improved fitting between the measured FRF and the FRF computed based on the updated material properties versus standard material damping data. The frequency accumulated L^2 norm between the measured and computed FRF's sums the distance separating the curves along the frequency range. The larger the accumulated error, the worse is the curve fitting through the frequency band. Bottom graph in fig.

5.9 shows that the measured versus computed mobility distance, which is accumulated through the frequency range, is much larger when using admittance coefficients calculated with standard material properties compared to updated parameters.

5.4 Conclusions

A 2-stage updating process based on the constitutive relation error technique was successfully tested and validated : it makes the CPU time slow down and allows an easy and costless comparison of different admittance models.
The CRE updating technique has been applied to the TRICARMO simplified concrete car to describe the absorbing materials of the seat of the driver. The pressure/exciting velocity ratio coming from the updating stage is compared to the experimental ratio at the driver's ear. The CRE technique, which minimizes the global error inside the whole acoustic domain, provides a quite good improvement of the computed FRF at the particular location where the updated and experimental FRF's are compared.

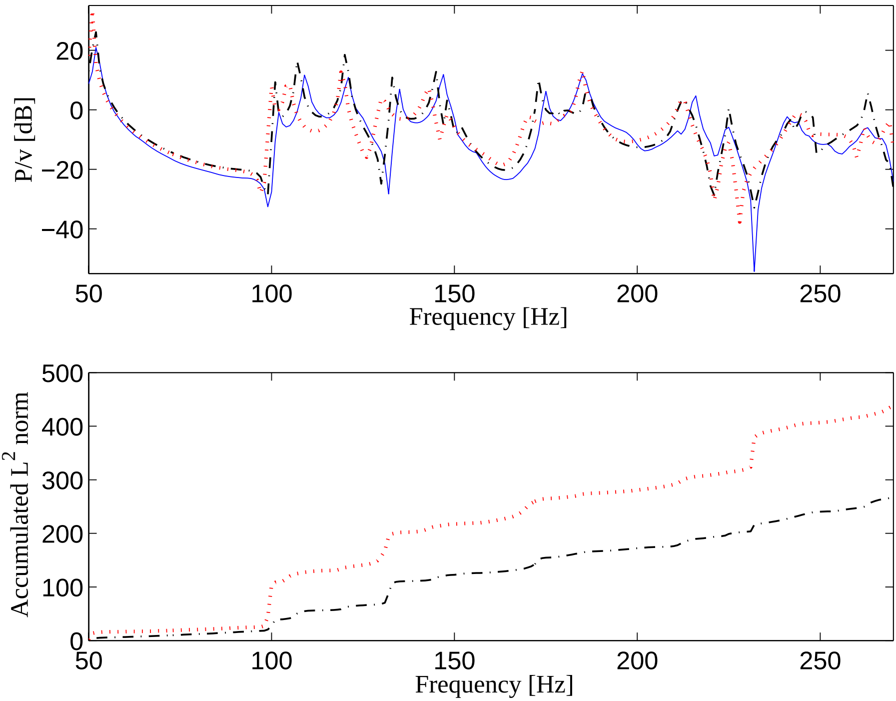

Figure 5.9: Top figure: mobility amplitude from 1) measured pressure (solid line), 2) computed pressure using updated A_n (dash-dotted line), 3) computed pressure using standard material properties (dotted line). Bottom figure: frequency accumulated error (L^2 norm) between measured and computed mobility using 1) updated A_n (dash-dotted line) 2) standard material properties (dotted line)

Chapter 6

Conclusions and perspectives

While the present work initially aimed at investigating the ability of the constitutive law error updating technique to improve the acoustic numerical model quality by the use of experimental data, the work soon started offering more and more opportunities in a quickly moving research area proposing many additional side developments potentially applicable to the acoustics.
Consequently, the concluding remarks are divided into two sections, the first one dealing with the main findings of the research so far, and the second part proposing a few recent theories to be considered for future works.

6.1 Major findings summary

Inspired by similar developments in structural dynamics, the constitutive law error (CLE) technique is successfully applied to acoustics. A first application on a bidimensional longitudinal cut of a car cabin demonstrates the ability of the method to update acoustic admittance coefficients covering several locations of the setup boundary. The admittance parameters are described in a frequency band in presence of measurement noise, and the error recorded on the updated coefficients is less or equal to the average noise level.

Knowing that the CLE updating technique deals with the improvement of given less reliable numerical model laws and does not count for additional error sources like for instance the discretization error (imprecise geometry approxi-

mation, dispersion error inherent to the Helmholtz equation), the effect of the numerical pollution on the model updating quality is examined.
In particular, the element-free Galerkin method (EFGM) and the usual finite element technique are used simultaneously to update the same model while increasing the frequency and controlling the dispersion error thanks to a highly refined reference model. It is shown that for mid frequencies, it is computationally more efficient to use an approximation method whose frequency behavior is more robust, the updating with the EFGM being significantly more effective then the classical FEM for increasing frequencies.

Then, the problem of updating large models is addressed and a dedicated reduction subspace is developed based on the re-writing of the updating system under the form of a set of undamped forced vibration problems. The reduced basis accounts for numerous contributions, namely a truncated modal basis and Krylov series, which are static responses of the system to the excitations and system variations during the updating process, but also vectors associated to the measured degrees of freedom.
Updating a 3D simplified car model of still rather small size ($\approx$ 1200 nodes) with the reduced basis increases the CLE level by less than 0.1% while the running time drops with a factor of 40 compared to the full model updating time. Simulations on a similar setup but using a refined mesh of about 20.000 nodes decreases the CPU time by a factor 110 compared to the non-reduced model.

Based on the CLE updating technique, a 2-stage process is implemented. The first stage makes the optimization procedure much easier by decreasing the number of parameters to be tuned when driving down the CLE estimator. The technique is developed in the particular case of updating acoustic admittance parameters whose frequency behavior can be described more or less accurately by using different models available in the literature. The 2-stage technique takes into account the admittance model formulation through the second stage only, which makes testing several admittance formulations when updating the acoustic setup costless, the second stage being very cheap.
The 2-stage formulation is applied to the TRICARMO simplified concrete car developed by LMS International. Available pressure measurements are used to improve the description of the driver's seat absorbing materials, decreasing the gap between measured and numerical frequency response function inside the car.

6.2 Perspectives/opportunities for enhancement

The most straightforward improvement of the implemented technique has to do with the optimization algorithm to be used when minimizing the CLE estimator with respect to the admittance parameters. Indeed, the choice of the optimization algorithm was not investigated into details through the dissertation. And it is not clear whether the mono-objective algorithm has to be global or if a local optimization process makes the deal. Most of the updating works performed during the study used a local minimization technique of gradient or simplex ([MN65]) type. Some trials with a genetic algorithm based global optimization technique ([FC04]) did not improve significantly the solution quality while obviously increasing the computational time.
In such a context, a systematic sensitivity study of the error estimator with respect to the coefficients of a given admittance model using for example a design of experiments (DOE) approach could improve the technique efficiency.

Additional future works could deal with vibro-acoustic model updating, the acoustic pressure field being potentially improved by updating the structural displacement of the surrounding boundary interacting with the fluid thanks to the coupling matrices, and vice-versa. So, the acoustic pressure updating could be performed thanks to accelerometers located on the structure instead of using microphones.

The Extended Constitutive Relation Error estimator proposed in [DLR04, LPDR06] for a family of quasi-identical structures in the context of uncertain experimental data could be applied to the acoustics. The measurements are described by a probability density function, and since very little statistical information is available, the authors use only the mean value for noise-free measurements from deterministic excitation. A probabilistic structural model is obtained by introducing uncertainties like material characteristics into the model parameters. The updating process then addresses validating a probabilistic model based on noisy measurements. The newly developed technique enables an engineer to quantify the quality of a given probabilistic model. The authors define a stochastic model to be exact if for any excitation the probability density function of the model solution equals the probability density function of the solution extracted from the experimental data set.

Other new concepts of interest were recently developed in [LPR06b, LPR06a] and define the notion of Lack Of Knowledge (LOK) in model validation. The goal is to be able to quantify the quality of a dynamic structural model by globalizing the various sources of errors on the substructure level by means of a scalar internal variable (the LOK variable). These variables are defined over an interval whose lower and upper bounds (the lower basic LOK and upper basic LOK) are described by a probability density function. The intervals, which are defined for each substructure, are then propagated rigorously throughout the mechanical model. Competing methods, which were developed by other authors [Dem68, Sha76], belong to the family of imprecise probabilities [Wal90] and are pretty similar.

Chapter 7

Acknowledgments

The scientific supervision of the present work was managed by Prof. Philippe Bouillard and Pierre Ladevèze, advisor and co-advisor of the thesis respectively. The time they spent in discussing the many topics of the dissertation gave its consistency to the set of works that were achieved during the four consecutive years of the PhD studies.

From a financial point of view, the funding of the Belgian organism for scientific research "Fonds pour la formation à la Recherche dans l'Industrie et dans l'Agriculture (FRIA)" is gratefully acknowledged.

Special thanks are addressed to Prof. Guy Warzée and Jean-Louis Migeot, members of the accompaniment comity of the thesis, who helped in keeping focused on the prime goals and drawing the conducting line of the work.

For the fruitful discussions and sharing his extended expertise in the CRE updating technique, Arnaud Deraemaeker was of unvaluable help. The staff of the Laboratoire de Mécanique et Technologie (Ecole Normale Supérieure, Cachan/Paris) has also to be acknowledged for its welcome during my stay there, the LMT being the nest of the CRE related developments. This study trip was founded by the Belgian "Fonds de la Recherche Scientifique".

From the industrial side, two Belgian companies collaborated on this project. The Free Field Technologies Company contributed to some numerical tests via the $ACTRAN^{\copyright}$ software that it develops. LMS International and especially Dr. E. Brechlin and H. Van der Auweraer successfully collaborated on the present work by providing the experimental data from the concrete car setup TRICARMO, which elaboration and all related test work were carried out in the framework of a Flemish research project financially supported by the

Flemish Institute for the promotion of scientific and technological research in industry (IWT).
In my new assignment within the Goodyear Tire & Rubber Company that followed my research fellowship, my gratitude goes to Dr. Didier Quoirin and Dany Assaker, immediate superiors in the computational mechanics department, who urged me to complete this document and made it possible by arranging my weekly schedule in allocating invaluable time to that task.
To my colleagues from the former ULB Structural and Material Computational Mechanics Department who shared my daily life during four years at the university, I express my warm thanks. More then co-workers, the sweet relationship driving the team was such that most if not all of the players became friends of mine.
In each and every project of our life, relatives are of the greatest importance because they are the confident to whom we turn in case of trouble. Thanks for providing me with a torch when, undergoing daily life darkness, I almost fell.
To anybody reading these lines and recognizing himself, I would like you to be proud of this work which is as much yours as mine, because we only exist through interactions we experience with others.

Bibliography

[AC92] J-F. Allard and Y. Champoux. New empirical equations for sound propagation in rigid frame fibrous materials. In *J. Acoust. Soc. Am.*, volume 91, pages 3346–3353, 1992.

[ADN+90] J.-F. Allard, C. Depollier, J. Nicolas, W. Lauriks, and A. Cops. Propriétés acoustiques des matériaux poreux saturés d'air et théorie de Biot (in french). In *Journal d'Acoustique*, volume 3, pages 28–38, 1990.

[All93] J.F. Allard. *Propagation of sound in porous media.* Elsevier Science Publishers LTD, 1993. ISBN 185166887.

[Att83] K. Attenborough. Acoustical characteristics of rigid fibrous absorbents and granular materials. In *J. Acoust. Soc. Am.*, volume 73, pages 785–799, 1983.

[BADM06] Ph. Bouillard, J.P.M. Almeida, V. Decouvreur, and T. Mertens. Some challenges in computational vibro-acoustics: verification, validation and medium frequencies. In *Computational Mechanics (accepted for publication)*, 2006.

[Bal96] E. Balmès. Parametric families of reduced finite element models, theory and applications. In *Mechanical Systems and Signal Processing*, volume 10 (4), pages 381–394, 1996.

[Bal97] E. Balmès. Garteur group on ground vibration testing: results from the test of a single structure by 12 laboratories in europe. In *IMAC*, pages 1346–1352, 1997.

[Bal98] E. Balmès. Efficient sensitivity analysis based on finite element model reduction. In *Proc. IMAC XVII, SEM, Santa Barbara, CA*, 1998.

[Bal00] E. Balmès. Review and evaluation of shape expansion methods. In *Proc, IMAC XVIII, San Antonio, Texas*, 2000.

[Bar82] M. Baruch. Optimal correction of mass and stiffness matrices using measured modes. In *AIAA Journal*, volume 20(11), pages 1623–1626, 1982.

[BB01] A. Bobillot and E. Balmès. Solving minimum dynamic residual expansion and using results for error localisation. In *Proc. IMAC XIX, SEM, Kissimee, Florida*, 2001.

[BBKD02] E. Brechlin, I. Bosmans, N. Keymeulen, and R. Dekkers. Experimental investigations of the vibro-acoustic behaviour of trim components in a car cabin. In *International Conference on Noise & Vibration Engineering, ISMA2002, Leuven, Belgium*, 2002.

[BI99] Ph. Bouillard and F. Ihlenburg. Error estimation and adaptivity for the finite element solution in acoustics: 2D and 3D applications. In *Comput. Methods Appl. Mech. Engrg.*, volume 176, pages 147–163, 1999.

[Bio56] M. A. Biot. Theory of elastic waves in a fluid saturated porous solid. II. Higher frequency range. In *J. Acoust. Soc. Am.*, volume 28, pages 179–191, 1956.

[BLC97] A. Bouazzouni, G. Lallement, and S. Cogan. Selecting a ritz basis for the reanalysis of the frequency response functions of modified structures. In *Journal of Sound and Vibration*, volume 2, pages 309–322, 1997.

[BM97] I. Babuška and J. Melenk. The partition of unity method. In *Int. J. Numer. Meth. Eng.*, volume 40, pages 727–758, 1997.

[BN83] A. Berman and J. Nagy. Improvement of a large analytical model using test data. In *AIAA Journal*, volume 21(8), pages 1168–1173, 1983.

[BS98] Ph. Bouillard and S. Suleau. Element-free Galerkin solutions for Helmholtz problems: formulation and numerical assessment of the pollution effect. In *Comput. Methods Appl. Mech. Engrg.*, volume 162, pages 317–335, 1998.

[Bui02] Z. Bui. Krylov subspace techniques for reduced order modelling of large-scale dynamical systems. In *Applied Numerical Math.*, volume 43, pages 9–44, 2002.

[Bur94] D. S. Burnett. A three-dimensional acoustic finite element based on a prolate spheroidal multipole expansion. In *J. Acoust. Soc. Am.*, volume 96, pages 2798–2816, 1994.

[Cae87] B. Caesar. Updating system matrices using modal test data. In S.E.M. London, England, editor, *Proc. IMAC V*, pages 453–459, 1987.

[CFN84] N. Cottin, H.P. Felgenhauer, and H.G. Natke. On the parameter identification of elastomechanical systems using input and ouput residuals. In *Ingenieur Archiv*, volume 54, pages 378–387, 1984.

[Cho97] A. Chouaki. *Recalage de modèles dynamiques de structures avec amortissement (in French).* PhD dissertation, Ecole Normale Supérieure de Cachan, 1997. ISBN 2-11-090977-3.

[CJZ91] Y. K. Cheung, W. G. Jin, and O. C. Zienkiewicz. Solution of Helmhotz equation by Trefftz method. In *Int. J. Numer. Meth. Eng.*, volume 32, pages 63–78, 1991.

[CLP97] A. Chouaki, P. Ladevèze, and L. Proslier. An updating method for damping in structural dynamic models. In *Proc. IMAC XV, Orlando, Florida*, pages 558–564, 1997.

[Com00] J.-Ph. Combe. *Sur le contrôle des calculs en dynamique rapide: application aux problèmes d'impact (in French).* PhD dissertation, Ecole Normale Supérieure de Cachan, 2000. ISBN 2-11-091681-8.

[CS92] Y. Champoux and M. Stinson. On acoustical models for sound propagation in rigid frame fibrous materials and the influence of shape factors. In *J. Acoust. Soc. Am.*, volume 92, pages 1120–1131, 1992.

[DB70] M. A. Delany and E. N. Bazley. Acoustic properties of fibrous absorbent materials. In *Appl. Acoust.*, volume 3, pages 105–116, 1970.

[DBB99] A. Deraemaeker, I. Babuška, and Ph. Bouillard. Dispersion and pollution of the FEM solution for the Helmholtz equation in one, two and three dimensions. In *Int. J. Numer. Meth. Eng.*, volume 46, pages 471–499, 1999.

[DBDL02] V. Decouvreur, Ph. Bouillard, A. Deraemaeker, and P. Ladevèze. Validation of acoustic models based on the constitutive relation error. In H.A. Mang, F.G. Rammerstorfer, and J. Eberhardsteiner, editors, *WCCM V Fifth World Congress on Computational Mechanics, Vienna, Austria.* Vienna University of Technology, 2002. ISBN 3-9501554-0-6, http://wccm.tuwien.ac.at.

[DBDL04a] V. Decouvreur, Ph. Bouillard, A. Deraemaeker, and P. Ladevèze. Updating 2D acoustic models with the constitutive relation error. In *Journal of Sound and Vibration*, volume 278(4/5), pages 773–787, 2004.

[DBDL04b] V. Decouvreur, Ph. Bouillard, A. Deraemaeker, and P. Ladevèze. Using a reduced modal basis to update acoustic models. In *IMACXXII Conference & Exposition on Structural Dynamics, Dearborn, USA*, 2004.

[DBVB05] E. De Bel, P. Villon, and Ph. Bouillard. Forced vibrations in the medium frequency range solved by a partition of unity method with local information. In *Int. J. Numer. Meth. Eng.*, volume 62, pages 1105–1126, 2005.

[DDBB05] V. Decouvreur, E. De Bel, and Ph. Bouillard. On the effect of the dispersion error when updating acoustic models. In *Comput. Methods Appl. Mech. Engrg.*, volume 195(2006), pages 394–405, 2005.

[DDLB06] V. Decouvreur, A. Deraemaeker, P. Ladevèze, and Ph. Bouillard. Building a suited reduced modal basis for updating 3D acoustic models with the constitutive law error method. In *Comput. Methods Appl. Mech. Engrg. (submitted for publication)*, 2006.

[Dem68] A.P. Dempster. Upper and lower probabilities generated by a random interval. In *Ann. Math. Statist.*, volume 39(3), pages 957–966, 1968.

[Der01] A. Deraemaeker. *Sur la maîtrise des modèles en dynamique des structures à partir de résultats d'essais (in French).* PhD dissertation, Ecole Normale Supérieure de Cachan, 2001. ISBN 2-11-093229-5.

[DLB06] V. Decouvreur, P. Ladevèze, and Ph. Bouillard. Updating 3D acoustic models with the constitutive law error method: a two-step approach for absorbing material characterization. In *Journal of Sound and Vibration (submitted for publication)*, 2006.

[DLL02] A. Deraemaeker, P. Ladevèze, and Ph. Leconte. Reduced bases for model updating in structural dynamics based on constitutive relation error. In *Comput. Methods Appl. Mech. Engrg.*, volume 191(21-22), 2002.

[DLR04] A. Deraemaeker, P. Ladevèze, and T. Romeuf. Model validation in the presence of uncertain experimental data. In *Engineering Computations*, volume 21-8, pages 808–833, 2004.

[DSK02] G. Dutilleux, F.C. Sgard, and U.R. Kristiansen. Low-frequency assessment of the in situ acoustic absorption of materials in rooms: an inverse problem approach using evolutionary optimization. In *Int. J. Numer. Meth. Engng*, volume 53, pages 2143–2161, 2002.

[DvHS02] W. Desmet, B. van Hal, and P. Sas. A computationally efficient prediction technique for the steady-state dynamics analysis of coupled vibro-acoustic systems. In *Advances in Engineering Software*, volume 33, pages 527–540, 2002.

[FC04] R. Filomeno Coelho. *Multicriteria Optimization with Expert Rules for Mechanical Design.* PhD dissertation, Université Libre de Bruxelles, 2004.

[FFML97] L. Franca, C. Farhat, A. Macedo, and M. Lesoinne. Residual-free bubbles for the Helmholtz equation. In *Int. J. Numer. Meth. Eng.*, volume 40, pages 4003–4009, 1997.

[FHF01] C. Farhat, I. Harari, and L. Franca. The discontinuous enrichment method. In *Comput. Methods Appl. Mech. Eng.*, volume 190, pages 6455–6479, 2001.

[FJT00] K.-Y. Fung, H. Ju, and B.P. Tallapraga. Impedance and its time-domain extensions. In *AIAA Journal*, volume 38, pages 30–38, 2000.

[Fre00] R. W. Freund. Krylov-subspace methods for reduced order modelling in circuit simulation. In *J. Comput. Appl. Math.*, volume 123, pages 395–421, 2000.

[Fre02] Free Field Technologies. *ACTRAN Rev.2.0 Users' Guide.* 2002.

[Fri86] C.P. Fritzen. Identification of mass, damping and stiffness matrices of mechanical systems. In Transaction of the ASME, editor, *Journal of Vibration, Acoustics, Stress and Reliability in Design*, volume 108, pages 9–16, 1986.

[GD96] K. Gerdes and L. Demkowicz. Solution of the 3D Helmholtz equation in arbitrary exterior domains using hp-fem and ifem. In *Comput. Methods Appl. Mech. Engrg.*, volume 137, pages 239–273, 1996.

[HH92] I. Harari and T. J. R. Hughes. Galerkin/least -squares finite element methods for the reduced wave equation with non-reflecting boundary conditions in unbounded domains. In *Comput. Methods Appl. Mech. Eng.*, volume 98(3), pages 411–454, 1992.

[IB95] F. Ihlenburg and I. Babuška. Finite element solution of the Helmholtz equation with high wave number. part 1: the h-version of the FEM. In *Comput. Math. Applic.*, volume 38(9), pages 9–37, 1995.

[IM90] D.J. Inman and C. Minas. Matching analytical models with experimental modal data in mechanical systems. In *Control and dynamic of systems*, volume 37, pages 327–363, 1990.

[JKD87] D.L. Johnson, J. Koplik, and R. Dashen. Theory of dynamic permeability and tortuosity in fluid-saturated porous media. In *J. Fluid Mech.*, volume 176, pages 379–401, 1987.

[KJL01] L. Kelders, G. Jansens, and W. Lauriks. Material parameter evaluation. In *Katholieke Universiteit of Leuven internal report, LMS P.V. 4351*, pages 1–13, 2001.

[Lad98] P. Ladevèze. A modelling error estimator for dynamic model updating. In *New Advances in Adapative Computational Methods in Mechanics*, pages 135–151, 1998.

[LARB01] P. Ladevèze, L. Arnaud, P. Rouch, and C. Blanzé. The variational theory of complex rays for the calculation of medium-frequency vibrations. In *Engineering Computations*, volume 18(1/2), pages 193–214, 2001.

[LBV03] V. Lacroix, Ph. Bouillard, and P. Villon. An iterative defect-correction type meshless method for acoustics. In *Int. J. Numer. Meth. Eng.*, volume 57(15), 2003. In press.

[LDLLB02] P. Ladevèze, A. Deraemaeker, S. Le Loch, and D. Barthe. A validation method of dynamic structural models: basic aspects and applications. In *Quanse 2002: International Congress on Quality Assessment of Numerical Simulations in Engineering, University of Concepción - Chile*, 2002.

[LPDR06] P. Ladevèze, G. Puel, A. Deraemaeker, and T. Romeuf. Validation of structural dynamics models containing uncertainties. In *Comput. Methods Appl. Mech. Eng.*, volume 195(4/6), pages 373–393, 2006.

[LPR06a] P. Ladevèze, A. Puel, and T. Romeuf. Lack of knowledge in structural model validation. In *Comput. Methods Appl. Mech. Eng.*, volume 195(37/40), pages 4697–4710, 2006.

[LPR06b] P. Ladevèze, A. Puel, and T. Romeuf. On a strategy for the reduction of the lack of knowledge (lok) in model validation. In *Reliability Engineering & System Safety*, volume 91(10/11), pages 1452–1460, 2006.

[LWB87] M. Link, M. Weiland, and J.M. Barragan. Direct physical matrix identification as compared to phase resonance testing: an assesment based on practical application. In S.E.M. London, England, editor, *Proc. IMAC V*, pages 804–811, 1987.

[MF93] J. Mottershead and M. Friswell. Model updating in structural dynamics: a survey. In *Journal of Sound and Vibration*, pages 347–375, 1993.

[MI68] P.M. Morse and K.U. Ingard. *Theoretical acoustics*. McGraw-Hill, Princeton, NJ, 1968.

[MKN02] S.V. Modak, T.K. Kundra, and B.C. Nakra. Comparative study of model updating methods using simulated experimental data. In *Computers & Structures*, pages 437–447, 2002.

[MN65] R. Mead and A. Nelder. A simplex method for function minimization. In *Computer Journal*, volume 7, pages 308–313, 1965.

[MO95] H. Morand and R. Ohayon. *Fluid-Structure Interaction*. John Wiley and Sons LtD, Chichester, England, 1995.

[Nat88] H.G. Natke. Updating computational models in the frequency domain based on measured data: a survey. In *Probalistic Engineering Mechanics*, volume 3(1), pages 28–35, 1988.

[Nef82] D.J. Nefske. Structural-acoustic finite element analysis of the automobile passenger compartment : a review of current practice. In *Journal of Sound and Vibration*, volume 80-2, pages 247–266, 1982.

[PGR98] R. Pascual, J.C. Golinval, and M. Razeto. On the reliability of error localization indicators. In *Proc. ISMA 23, Leuven, Belgium*, 1998.

[Qu01] Z. Qu. Accurate methods for frequency responses and their sensitivities of proportionally damped systems. In *Computers&Structures*, volume 79, pages 87–96, 2001.

[RR00] P. Rohl and G. Reese. Salinas - an implicit finite element structural dynamics code developed for massively parallel platforms. In *American Institute of Aeronautics and Astronautics*, pages 1651–1660, 2000.

[SB00] S. Suleau and Ph. Bouillard. 1-D dispersion analysis for the element-free Galerkin method for the Helmholtz equation. In *Int. J. Numer. Meth. Eng.*, volume 47, pages 1169–1188, 2000.

[Sha76] G. Shafer. *A mathematical theory of evidence.* Princeton, NJ, Princeton University Press, 1976.

[TA99] M.A. Tournour and N. Atalla. Efficient evaluation of the acoustic radiation using multipole expansion. In *Int. J.Num. Meth. Engrg.*, volume 46 (6), pages 825–837, 1999.

[Tar87] A. Tarantola. *Inverse problem theory, methods for data fitting and model parameter estimation.* Elsevier, Netherlands, 1987.

[Vor96] N. Voronina. Improved empirical model of sound propagation through a fibrous material. In *Appl. Acoust.*, volume 48-2, pages 121–132, 1996.

[Vor97] N. Voronina. An empirical model for rigid frame porous materials with high porosity. In *Appl. Acoust.*, volume 51-2, pages 181–198, 1997.

[Vor98] N. Voronina. An empirical model for elastic porous materials. In *Appl. Acoust.*, volume 55-1, pages 67–83, 1998.

[Wal90] P. Walley. *Statistical reasoning with imprecies probabilities.* London, Chapman & Hall, 1990.

[Wil97] D.K. Wilson. Simple, relaxational models for the acoustical properties of porous media. In *Appl. Acoust.*, volume 50-3, pages 171–188, 1997.

[ZW90] D.C. Zimmerman and M. Widengren. Correcting finite element models using a symmetric eigenstructure assignement technique. In *AIAA Journal*, volume 28(9), pages 1670–1676, 1990.